POLITECNICO DI MILANO

School of Information and Industrial Engineering
Electronic, Information and Bioengineering Department
Master of Science in Telecommunications Engineering

Diffusive MIMO Molecular Communication Systems

Author: Seyed Mohammadreza Rouzegar ID: 840698

Supervisor: Prof. Umberto Spagnolini

July 2017

Dedication

I dedicate this thesis to my family: Mansour, Azita, Maryam and Arya. You have always supported me with your unending love. I love you so much.

I specifically thank Prof. Spagnolini for supporting me during this thesis. His consultancy was a precious to me and I declare that without him this thesis would not exist.

I thank all my colleagues at Vodafone specially Alessandro, Giovanni, Andrea and etc. Alessandro it was really amazing working with you.

I thank all my friends who supported me during this thesis. Andrea and Lorenzo, we had an amazing time at EuCNC conference at Oulu. Shahin, Saeed, Milad, Reza, Amjad, Maryam and etc. I thank all of you and other friends who have been with me this year.

And finally, I thank my uncle Jafar, who has always supported me. Your friendship is valuable to me and I have learned many things from you.

Contents

List of Figures

List of Tables

List of Abbreviations

BER	Bit Error Rate
BL	Blind Equalization
CIR	Channel Impulse Response
CRB	Cramér-Rao Bound
CSI	Channel State Information
CSK	Concentration Shift Keying
D-MIMO	Diffusive MIMO
DFE	Decision Feedback Equalizer
ILI	Inter-Link Interference
ISI	Inter-Symbol Interference
LSD	Least Squares Detector
LS	Least Squares
MC	Molecular Communication
MIMO	Multiple-Input Multiple-Output
ML	Maximum Likelihood

MSE	Mean Squared Error
PDF	Probability Density Function
SISO	Single-Input Single-Output
TIL	Time Interleaving

Abstract

In diffusion-based communication, as for molecular systems, the achievable data rate is very low due to the slow nature of diffusion and the existence of severe inter-symbol-interference (ISI). Multiple-input multiple-output (MIMO) technique can be used to improve the data rate. MIMO technique cause inter-link interference (ILI) in addition to the the ISI. MIMO time interleaving (TIL) modulation technique is introduced at the transmitter to mitigate the ILI. Knowledge of channel impulse response (CIR) is essential for equalization and detection in MIMO systems. This thesis presents a training-based CIR estimation for diffusive MIMO (D-MIMO) channels. Maximum likelihood and least-squares estimators are derived, and the training sequences are designed to minimize the corresponding Cramér-Rao bound. Sub-optimal CIR estimators are compared to the Cramér-Rao bound to validate their performance. Also, several equalization and detection schemes are proposed to investigate the performance of the D-MIMO MC system. We have studied the effect of the D-MIMO system parameters in terms of bit error rate (BER) and throughput when channel state information (CSI) is available at the receiver. Finally, block-type communication is assumed and designed training sequences are transmitted at the beginning of each block for CIR estimation. Then, estimated CIR is used during the rest of the block to equalize the received signals for detection. The effect of training sequence length on BER and throughput is studied and it is shown that for short training sequence length, system performance reach to the ideal case when CSI is available at the receiver.

Abstract (Italiano)

Nei sistemi di comunicazione basati su canali di tipo diffusivo, come nel caso di sistemi molecolari, il massimo ritmo di trasmissione raggiungibile è limitato dalla lenta natura della diffusione e dall'esistenza di una severa interferenza intersimbolica (ISI). Sistemi di comunicazione che utilizzano una schiera di antenne sia al trasmittitore che al ricevitore (MIMO) posso essere utilizzati per migliorare il ritmo di trasmissione. Tuttavia, i sistemi MIMO, oltre all'ISI, introducono ulteriore interferenza tra i vari canali spaziali (ILI). Quest'ultima può essere mitigata utilizzando tecnica di interleaving nel tempo. La conoscenza della risposta all'impulso del canale (CIR) è fondamentale per l'equalizzazione e la rivelazione nei sistemi MIMO. Questa tesi presenta una tecniche di stima della CIR per canali MIMO diffusivi (D-MIMO) basata su sequenze di training. Stimatori a massima verosimiglianza (ML) e ai minimi quadrati (LS) sono stati derivati per la stima delle CIR e le sequenza di training sono state ottimizzate per minimizzare il corrispondente limite di Cramer-Rao. Le prestazioni di stimatori delle CIR sub-ottimi sono stati confrontati con il limite di Cramer-Rao per validarne l'efficacia. In più, varie tecniche di equalizzazione e rivelazione sono state proposte per analizzare le prestazioni dei sistemi D-MIMO molecolari. I parametri che caratterizzano i sistemi D-MIMO sono stati studiati in termini di probabilità d'errore sul bit (BER) a ritmo di trasmission nel caso in cui si assume completa conoscenza del canale (CSI) al ricevitore. Infine, la comunicazione a blocchi è stata enorcare con le sequenze di training che trasmesse all'inizio di ogni blocco per la stima delle CIR. Tali CIR stimate sono poi utilizzate per equalizzare e rivelare i segnali ricevuti per la rimanente durata del blocco. L'impatto della lunghezza delle sequenze di training sulla probabilità di errore sul simbolo e sul ritmo di trasmissione è stata studiata, dimostrando che anche per sequenza di lunghezza relativamente corta, le prestazioni del sistema approcciano il caso ideale in cui il ricevitore dispone di una perfetta conoscenza delle infromazioni di canale.

Chapter 1

Introduction

Molecular communication (MC) is a bio-inspired solution of communication at nano-scale [1, 2, 3, 4, 5, 6]. Conventional communication systems transfer information using electromagnetic waves. At nano-scale, antennas suffer the constraint of being at comparable scale of electromagnetic wavelength. Additionally, using electromagnetic wave for nanomachines can be detrimental in some environments, such as inside a body where electromagnetic radiation can be harmful for health. Hence, MC can be a preferred solution for communication among nanomachines to build a nanonetwork, so they can perform complex tasks which could not be possible individually [7, 8, 9].

There are many potential applications considered for MC at micro-scales, such as medical application and communication between nanorobots. The continuous advances in nanotechnology, e.g. nanomachines and nanorobots, let us think about devices at nano-scale that are capable of communication and computation [10]. Indeed, one of the main interesting application of MC in medicine is artificial immune system [11], where many minuscule devices are injected to the body. Each tiny device is engineered for a specific task with a limited functionalities. However, They can build a big nano-network to carry out complex tasks such as targeted drug delivery [12] and cancer treatment [13].

In nature, MC is employed over short-range (nm scale), mid-range (μm to cm scale), or long-range (cm to m scale) communication. For example, neurotransmitters use passive transport (free diffusion) to communicate over shortrange; inside cells, motor proteins are used to actively transport cargoes over the mid-range; and hormones are transported over the long-range using flow (e.g., blood flow from the heart). In this thesis we refer to the short-

and mid-range as microscale MC, and the long-range as macroscale MC. The physical properties of matter change from macroscales to microscales, hence we consider each of them separately.

In MC, bio-nanomachines communicate through exchanging molecules through an aquas environment. In fact, the simplest system needs a transmitter to send the information molecules, and a receiver to collect them. In the following, we briefly introduce each part of the MC system.

1.1 MC Transmitters

Transmitters in MC systems release information molecules into the aquas or gaseous environment. According to the considered range of communication, transmitter architectures would be different.

1.1.1 Micro-scale MC Transmitters

The transmitter is a bio-nanomachine which can be generated by genetically modified cells [14], artificial cells [15] or also can be a nanorobot. Any transmitter at least needs a unit for storage of information molecules and a processing unit to encode the data by controlling the gates. The processing unit can be synthesized by logic gates and memory into cells as shown in [16, 17]. The information particles can be generated by modifying a metabolic pathway of a biological cell, which then synthesizes and releases specific signaling molecules [17]. Transfection, transfer via viral vectors, direct injection to germ line, and transfer via embryonic stem cells are the methods for gene transfer for modifying a metabolic pathway [18, 19]. Among these methods, viral vectors are a commonly used tool by molecular biologists to deliver genetic material into cells. This process is used for manipulating a living cell to engineer regulatory networks that can be used for communication. Viruses efficiently transport their genomes inside the cells they infect for desired function. Main types of viral vectors are retroviruses, lentiviruses, adenoviruses, adeno-associated viruses, and nanoengineered substances [20].

To control the release timing, a synthetic oscillator can be introduced into a cell [21, 22], which with the help of the central processing unit acts as the release control module. Therefore, it is possible to have all the components of a transmitter synthesized into cells.

1.1.2 Macro-Scale MC Transmitters

At macroscales, the transmitter requires the same units as the micro-scale transmitters but their realization are different. For the transmitter, a storage container is required for holding the information particles. It is also possible to generate the information particles using different processes. A mechanism must be set in place for controlled release of molecules. For example, sprays could be used for controlling the release of information particles. In [23, 24], a technique for releasing complex blends of compounds in specific ratios, which mimics insect pheromones, is developed.

The processing unit at macroscales can be a computer or a microcontroller, depending on the application. The power source could be electrical, solar, or any other source. At macroscales, different power sources and processing unit have already been well studied and developed.

In this paper we have assumed a storage full of information molecules. According to the information to be transmitted, we keep the gates closed or open them shortly at the beginning of bit interval time. Molecules flow out when the gate is open due to the concentration difference inside and outside of the storage . By controlling the gates opening time and their size, we can encode the input signal to the different properties of molecules, such as their concentration [25], number [26], type [27], and time of release [28, 29]. Information molecules can be any type of molecules according to the application and also it can be synthesized for drug delivery applications.

In this thesis, we have assumed that information is encoded in the number of molecules. We have also assumed ON-OFF key signaling, means that for signaling the bit one, we open the gate and for signaling the bit zero, we keep the gate closed. Fig. (1.1) shows the simplified diagram of the MC transmitter for a 2×2 D-MIMO system. There are two independent gates where it is assumed we have full control of their size and timing, so we can control the number of released molecules at each bit interval time at each gate. Gates resemble antennas in conventional communications, so for the rest of the paper we refer them as antennas for simplicity.

1.2 MC Receivers

MC receivers should have at least a detection unit to sense the information molecules and a processing unit to decode the data. According to the range of communication, the configuration of the receivers are different. In the following

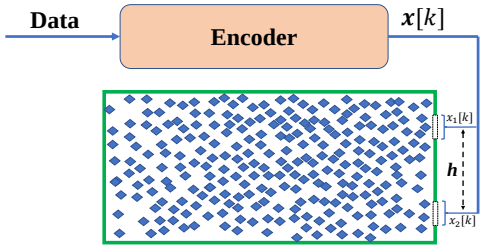

Figure 1.1: Transmitter of a 2×2 D-MIMO system. The encoder controls the gates opening time and aperture size. In case of ON-OFF key signaling, for signaling the bit one, the encoder open the gate, and for signaling the bit zero, keeps it closed. Molecules flow out due to the concentration difference inside and outside of the storage. The gate aperture size and opening time controls the number of released molecules in each bit interval time.

we explain MC receiver at micro- and macro-scale.

1.2.1 Micro-scale MC Receivers

In nature, signals are received via protein structures called receptors. Therefore, these protein structures can be seen as receiving antennas. Receptors are the special protein structures that can bind to specific ligand structures. The binding occurs by intermolecular forces, such as ionic bonds, hydrogen bonds and van der Waals forces. Ligand binding to a receptor alters the receptor's chemical conformation and the tendency of binding is called affinity. The conformational state of a receptor determines its functional state [30]. Most receptors remove the information molecules from the environment through binding, absorbing, or chemical reactions. Therefore, in most cases almost all the molecules contribute to the signal at most once [30].

Cells can also be created artificially by using liposome vesicles as the membrane encapsulating different functional proteins that together carry the task of the central processing unit, the particle generation and storage unit, receptors, and the particle release control unit for the transmitter and the receiver.

1.2.2 Macro-scale MC Receiver

For detection at macro scale, chemical sensors can be used to detect the information particles. For example, metaloxide gas sensors [31] are typically inexpensive sensors, that are capable of detecting the concentration of various types of volatile chemicals and gases. It is also possible to create more sophisticated sensors for detecting mixture of chemicals as shown in [32].

1.3 MC Channel

The channel is the environment in which the transmitted signal propagates from the source to the receiver. In a traditional communication system, a channel is typically a wire or free space where the transmitted signals are the electrical currents or electromagnetic waves, respectively. In MC, small particles called information particles act as chemical signals conveying the information. Information particles are typically a few nanometers to a few micrometers in size. Information particles could be biological compounds, such as proteins, or synthetic compounds, such as gold nano particles. The channel in MC is an aqueous or a gaseous environment where the tiny information particles can freely propagate.

Information molecules can be transported by different propagation mechanism such as diffusion [33, 34, 35], flow assisted diffusion [26], active transport using molecular motors and bacterial assisted propagation [36, 37, 38]. In this thesis, diffusion-based communication is assumed where information molecules diffuse toward the receiver using Brownian motion resulting from their collision with the molecules in the fluid. Diffusion does not need any external energy and it uses the existing thermal energy that is already present in the environment, so it is very energy efficient.

1.4 Thesis Outline:

The outline of the thesis are as follows.

In chapter 2, we briefly talk about the history of molecular communications then we explain the current challenges at MC jargon. Then we mention the related published works and finally we remark the contribution of this thesis.

Chapter 3 describe the fundamentals of the diffusion phenomena and it investigates important diffusion parameters and discusses the diffusion behavior.

In Chapter 4, we present the system model for a single-input and single-output MC system. Then, MIMO system model is introduced and the algebraic notation is presented.

Chapter 5 presents the CIR estimation for Poisson channel of a $M \times M$ D-MIMO MC systems. Maximum likelihood (ML) and least squares (LS) CIR estimators are proposed and their performances are compared with the Cramér-Rao bound (CRB).

Chapter 6 presents equalization and detection techniques for the proposed D-MIMO systems. Maximum likelihood detection is developed with blind and decision feedback equalizers. Finally least squares detector (LSD) based on decision feedback equalizer is introduced.

In Chapter 7, a MIMO time interleaving modulation technique has been developed and it reduces the ILI and improves the performance.

In chapter 8, we present block-type D-MIMO molecular communication and we investigate the D-MIMO performance as throughput of the system for different equalizers and detectors proposed in this thesis.

1.5 Publications

• S. Mohammadreza Rouzegar, Umberto Spagnolini. "Channel Estimation for Diffusive MIMO Molecular Communication" Networks and Communications (EuCNC), 2017 European Conference on. IEEE, 2017 , Oulu, Finland.

• S. Mohammadreza Rouzegar, Umberto Spagnolini. "Practical Diffusive MIMO Molecular Communication" To be submitted

Chapter 2

Literature Review and Contributions

In this chapter we will focus on the history and evolution of molecular communications and its recent advancement. Then we focus on each part of the MC system including channel, receiver and transmitter. We investigate deeply each part of the system of the related works in the literature. Then we explain some existing challenges in the MC system and elaborate how MIMO technique can address the challenges. Finally, we will point out the contributions of this thesis to the molecular communication world.

2.1 History of Molecular Communications

In 2005 T. Suda et al. published the paper [39] "Molecular Communication" and they introduced the MC as an interdisciplinary research area that spans nano-technology, bio-technology and communication technology. They proposed that MC can be used to communicate between nanomachines. MC is inspired by observing that biological systems communicate through molecules. For example, biological systems perform intra-cellular communication through vesicle transport, inter-cellular communication through neurotransmitters and inter-organ communications through hormones. They pictured the molecular communication as mechanism between nanomachines to communicate over short distances (nanometers to micrometers) by means of molecules propagation. In the same year they published two other works [1, 2] investigating the challenges and possible applications on MC jargon. They described that nanomachines are small devices or components that are capable of performing

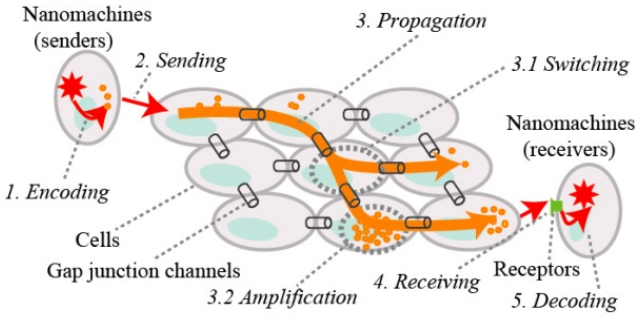

Figure 2.1: Molecular communication through gap junction channels [40]

only very simple tasks of computation, sensing, or actuation (e.g., detection of molecules, generation of motion, or performing chemical reactions) because of their limited size and limited complexity. Some examples of nanomachines in biological systems include molecular motors that produce motion or a receptor that reacts to specific molecules. Examples of artificial nanomachines include nanomachines synthesized using NEMS (Nanoelectro- mechanical Systems) technology from organic and/or artificial components at the submicron dimension. They introduced two MC design system using molecular motors and calcium signaling. One year later in 2006, they published two paper describing in details the two MC design system mentioned above.

In [41], authors described a molecular motor communication system. They proposed that by advancement of nanotechnology, nanomachines can communicate through MC and they build a nanonetwroks so they can performs complex tasks. They described molecular motors (e.g. kinesin, dynein) as a transport materials (e.g. vesicle, mRNA) in eukaryotic cells along filaments called rail molecules (e.g. microtubules). They proposed to develop a MC system where molecular motors are used for controlled nanomachine communication. In their proposed system, rail molecules (microtubules) are deployed between nanomachines, and molecular motors (kinesin) carry vesicles containing information molecules along the rail molecules from sender nanomachines to receiver nanomachines. The destination may be specified by a protein tag that binds to specific receptors on receiver nanomachines.

In 2007, the authors of [40] explored the design of a biological cell-based molecular communication system inspired by cell-cell communications through gap junction channels. Nanomachines in this scheme are engineered organisms

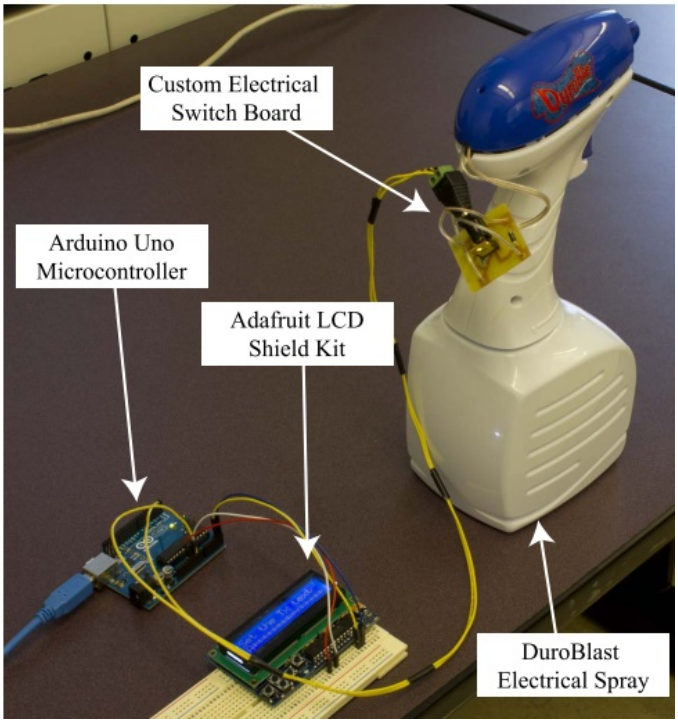

Figure 2.2: The transmitter architecture of a tabletop Molecular Communication system [44]

or biological devices whose behavior is programmed to achieve application specific goals, and chemically communicate over a cell-cell communication medium as depicted in Fig. 2.1.

In 2007 Andrew W.Eckford published a paper with different approach focusing on the communication and engineering aspect of the MC systems [42]. He proposed a model where information is encoded in the time and number of released molecules by transmitter. He assumed molecules have a random Brownian motion and he used information theory to calculate the capacity bound of the system according to his model. In [43] Dr. Eckford estimated the achievable information rates for a molecular communication system when information is encoded using a set of distinct molecules and they propagate across the medium via Brownian motion. His results indicated large gains in information rate over the case where the released molecules are indistinguishable from each other.

In [44] authors introduced the first modular, and programmable platform

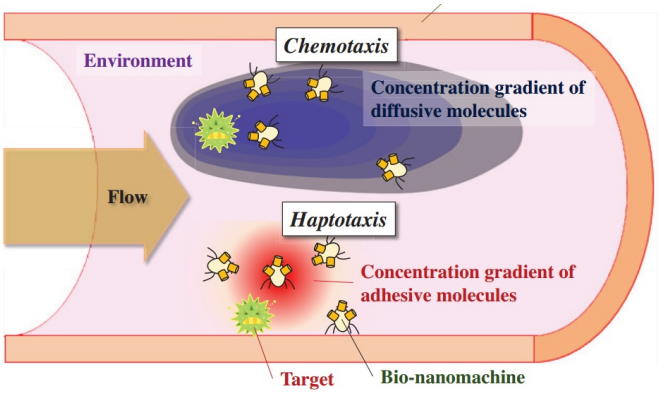

Figure 2.3: The mobile bio-nanosensor network [45]

capable of transmitting a text message using molecular communication. They implemented a macroscopic molecular communication system for transmitting a brief text message using chemical signals. Their proposed inexpensive and compact system requiring no supporting hardware or surrounding laboratory infrastructure.

Authors of [45] demonstrated an application of MC to an inbody mobile bionanosensor network as shown in Fig. 2.3. They explained that in the inbody mobile bionanosensor network, bio-nanomachines migrate in the environment while they release adhesive molecules that bind to a surface in the environment. The concentration gradient of adhesive molecules is thus formed over the surface, and bio-nanomachines migrate based on the gradient to coordinate their behavior. In the nondiffusion-based molecular communication, the formation of concentration gradient of adhesive molecules relies on the mobility of bio-nanomachines and thus the effective communication range may be limited. However, the non-diffusion-based molecular communication can maintain a high and stable concentration of molecules in the environment, allowing bio-nanomachines to detect the concentration to coordinate their behavior. Authors showed that non-diffusion-based molecular communication may apply to induce coordinated behavior among mobile bio-nanomachines in the inbody environment.

There are many papers focused on the biological aspects and possible application of the MC systems [12, 13, 11]. Also, there are other papers focusing on the communication and engineering aspects of MC such as [35, 46, 47, 26, 48, 49, 50, 51, 52, 53]. This thesis is focused on the engineering aspects of communication between nanomachines using diffusive channels. In the follow-

ing we will discuss about the diffusive channel, designing MC transmitters and receivers and we mention most relevant works in the literature.

2.2 Related Works

In this section we will investigate the communication engineering aspect of molecular communication. We can not mention all the related works due to the space constraints, but we will study the most relevant works to this thesis.

In [54], authors developed a communication system focusing on the release of either one or two molecules into a fluid medium with drift. They analyze the mutual information between transmitter and the receiver when information is encoded in the time of release of the molecule. They made some simplifying assumptions in order to calculate the mutual information. They calculated the upper bounds on the true mutual information. In their model they assumed the transmitter encodes the message in the time of release and possibly the number of molecules. Based on the number and the time of absorption of the molecules, the receiver decodes the transmitted information. They developed the mutual information between the transmitter and receiver for two cases: with a single transmitted molecule and two molecules whose release times can be chosen independently. For a given information transmission strategy at the transmitter (called the input distribution in the information theoretic literature), the mutual information is also the maximum rate at which information may be conveyed using that strategy. (Mutual information is related to but distinct from the capacity, which is the maximum mutual information over all possible input distributions.) In [55], authors compared and analyzed both propagation schemes by deriving a set of analytical and mathematical tools to measure the achievable information rates of the on-chip molecular communication systems employing passive to active transport.

Authors of [34] proposed a new molecular modulation scheme for nanonetworks. They assumed a Poisson diffusive channel to evaluate their modulation method with concentration and molecular shift keying. In concentration shift keying (CSK) symbols are encoded in the number of molecules released in each time slot and it is inspired by the Amplitude Shift Keying (ASK) used in the classical communication. Molecular Shift Keying (MOSK) scheme resembles the Frequency Shift Keying (FSK) in the classical communications. To transmit b bits per time slot, 2b different molecule types are utilized. The transmitter releases a specified number of molecules of the type corresponding to the current input symbol. To decode the transmitted signal at a certain

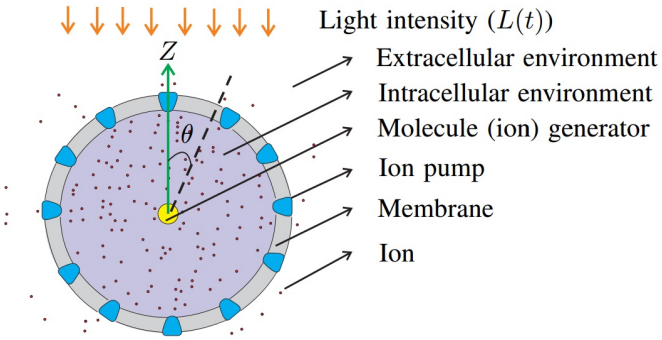

Figure 2.4: Schematic illustration of ion pump modulator [56]

time slot, the receiver looks for a unique molecule type whose concentration exceeds a certain threshold τ. An error occurs if the concentration of none of the molecule types or more than one molecule type exceeds τ. Interference due to the previous transmission in MOSK is less than that in the CSK. Authors proposed Molecular-Concentration Shift Keying (MCSK) inspired by previous modulation schemes where two types of molecules A1 and A2 are used; The transmitter uses type A1 in odd time slots, and type A2 in even time slots. To convey information in each time slot, different diffusion rates are used (similar to CSK). Thus, to match each symbol to b bits, 2b different propagation rates are utilized in each time slot. As the molecule types are different in two subsequent time slots, (i) the previous symbol interference is drastically reduced (ii) the decision threshold of the current symbol is independent of the last decoded symbol. Since the data is not encoded in the molecule types (but in the concentrations), the number of molecule types (and as a result the complexity), does not increase with b.

In [56] authors proposed a modulator based on ion pumps for diffusive MC where release rate of the molecules is controlled by modulating a light intensity signal (Fig. 2.4). The pumping process of the ion pump is modeled by a Markov model based on which the stochastic nature of the modulated signal, i.e., the release rate of the ions from the transmitter is analyzed. A simple on-off keying modulation scheme is realized based on the proposed modulator. They showed that a realistic transmitter can not release ions instantaneously nor deterministically.

In [57], authors propose a symbol interval optimization algorithm in molecular communication with drift. Proper symbol intervals are important in practical communication systems since information needs to be sent as fast as possi-

ble with low error rates. There is a trade-off, however, between symbol intervals and inter-symbol interference (ISI) from Brownian motion. They investigated an isomer-based molecule shift keying (IMoSK) modulation and calculated the achievable data transmission rates. They compared the normalized achievable rates for the one-symbol ISI and no ISI systems.

Authors of [58] presented the foundation of a multi-scale stochastic simulator from the perspective of molecular communication, for both mesoscopic and hybrid models. The multi-scale models use subvolumes of different sizes, between which diffusion event transition rate are derived. They showed the accuracy and efficiency of their approach outperforms the traditional approaches with that of a regular hybrid method.

In [33] authors added one new term to Fick's law related to relaxation of particles inspired by the statistical mechanics of electrons in heat diffusion. Therefore, they obtained the Telegraph equation for the diffusion of particles which is analytically equivalent to the wave equation in a lossy medium and the solution is well known. The green function of the telegraph equation is the analytical solution for the concentration evolution in space and time.

In [59], authors considered a multi-hop molecular communication network consisting of one nanotransmitter, one nanoreceiver, and multiple nanotransceivers acting as relays. They considered three different relaying schemes to improve the range of diffusion-based molecular communication. In the first scheme, different types of messenger molecules are utilized in each hop of the multi-hop network. In the second and third scheme, they assumed that two types of molecules and one type of molecule are utilized in the network, respectively. Authors considered two relaying modes analogous to those used in wireless communication systems, namely full-duplex and half-duplex relaying. They proposed the adaptation of the decision threshold as an effective mechanism to mitigate self-interference and backward-ISI at the relay for full-duplex and half-duplex transmission. They derived the closed-form expression for the expected end-to-end error probability of the network for the three considered relaying schemes. They also provided the closed-form expression for the optimal number of molecules released by the nanotransmitter and the optimal detection threshold of the nanoreceiver for minimization of the expected error probability of each hop.

In [60], authors reminded the importance of channel state information (CSI) to analyze the diffusive molecular communication systems. They studied the local estimation of channel parameters for diffusive molecular communication when a transmitter releases molecules that are observed by a receiver. They de-

rived the Fisher information matrix of the joint parameter estimation problem to calculate the Cramér-Rao bound on the variance of locally unbiased estimators. They reduced the joint estimation problem to the estimation of any subset of the channel parameters. They showed therein Maximum likelihood estimation leads to closed-form solutions for some single-parameter estimation problems and can be determined numerically. Peak-based estimators are proposed for low-complexity estimation of a single unknown parameter.

Farsad et al. developed a tabletop molecular communication platform for transmitting short text messages across a room in [61]. The end-to-end system CIR for this platform does not follow analytical published works because of imperfect receiver, transmitter, and turbulent flows. They introduced an end-to-end system impulse response based on the observed data from experimentation. Using the corrected impulse response models, they formulated the nonlinearity of the system as noise and showed that it can be represented as Gaussian noise.

Ian F. Akyildiz et al. studied and modeled the noise sources in ligand-binding reception for MC in Nanonetworks in [62]. They modeled the reception noise through the ligand-receptor kinetics and through the stochastic chemical kinetics. The ligand-receptor kinetics allows to simulate the random perturbations in the chemical processes of the reception, while the stochastic chemical kinetics provides the tools to derive a closed-form solution to the modeling of the reception noise. They expressed the ligand-receptor kinetics model through a block scheme, while the stochastic chemical kinetics results in the characterization of the reception noise using stochastic differential equations.

R. Schober et al. presented a training-based CIR estimators in [35] for single-transmitter single-receiver diffusive MC systems that estimate the CIR based on the observed number of molecules at the receiver due to emission of a sequence of known numbers of molecules by the transmitter. They considered two scenarios depending on whether or not statistical channel knowledge is available. In particular, they derived maximum likelihood (ML) and least sum of square errors (LSSE) estimators which do not require any knowledge of the channel statistics. For the case, when statistical channel knowledge is available, they proposed maximum a posteriori (MAP) and linear minimum mean square error (LMMSE) estimators. They derived the classical Cramér-Rao bound. Finally, they proposed an optimal and suboptimal training sequence design for the considered MC system.

U. Mitra et al. proposed in [48] a simple memory-limited decoder and showed therein that its performance reaches the best possible imaginable de-

coder (without any restrictions on the computational complexity or its functional form), using Genie-aided upper bounds. they showed that a four-bits memory achieves nearly the same performance as infinite memory. They considered a threshold decoders and demonstrated that system performance reaches the optimal decoder for high SNR values in a Poisson channel with memory. They proposed a multi-read system and showed therein that it can significantly improve the system performance. The associated decision rule for this system is shown to be a weighted sum of the samples during each symbol interval.

In [26] authors investigated receiver design for the SISO diffusive MC system. They considered diffusion with flow in any direction and using enzymes in the propagation environment to mitigate inter-symbol interference. They characterized the mutual information between receiver observations to investigate the observations independence. They derived the maximum likelihood sequence detector to provide a lower bound on the bit error probability and they used Viterbi algorithm to reduce the computational complexity of the optimal joint detection . They also proposed weighted sum detectors and derived their expected bit error probability. They showed the performance of the optimal weighted sum detector is equivalent to a matched filter.

B. Akan et al. investigated the receiver design in MC systems in [50]. They highlighted the effect of inter-symbol interference (ISI) on the performance of the system. They proposed four methods for a receiver in the MC to recover the transmitted information distorted by both ISI and noise. They introduced sequence detection methods based on maximum a posteriori (MAP) and maximum likelihood (ML) criterions, a linear equalizer based on minimum mean-square error (MMSE) criterion, and a decision-feedback equalizer (DFE) which is a nonlinear equalizer. They presented a channel estimator to estimate time varying MC channel at the receiver. They evaluated the performances of the proposed methods on the bit error rates. They showed therein that sequence detection has the best performance at the expense of computational complexity. However, the MMSE equalizer has the lowest performance with the lowest computational complexity.

Authors of [51] proposed three detector architecture for SISO MC system. They presented a low-complexity one-shot optimal detector to maximize the mutual information and a near Maximum Likelihood (ML) sequence detector. They showed that the one-shot detector achieves near-optimal throughput without the need of a priori information which suggests an ML sequence detector with high complexity is not necessary. They proposed a receiver design

which operates without failure even in the case of infinite channel memory.

In [52] authors remarked the importance of ISI mitigation for secure data transmission. They proposed a low-complexity and non-coherent signal detector, which exploits essentially the local convexity of the diffusive channel response. They presented a threshold estimator that detects signals blindly, which can also adapt to channel variations. They presented an algorithm that is capable of operating at high data rates and suppressing ISI from a large number of previous symbols. They showed that their proposed detector suppresses ISI and keep the detector architecture simple enough to be implemented on nanomachines.

In [49] authors studied a non-coherent multiple-symbol detection schemes which do not require knowledge of the CSI. In particular, they derived the optimal maximum likelihood (ML) multiple-symbol (MLMS) detector. They proposed an approximated detection metric and a suboptimal detector to cope with the high complexity of the optimal MLMS detector. Authors showed their proposed optimal and suboptimal detection schemes is so effective compare to the case where CSI is available, particularly when the number of observations used for detection is sufficiently large.

Authors of [63] designed codes which facilitate maximum likelihood sequence detection at the receiver without instantaneous or statistical CSI knowledge so they can prevent large overheads for CSI estimation. In particular, they demonstrated that strongly constant weight (SCW) codes, enables optimal CSI-free sequence detection at the cost of decreasing the data rate. They showed that their proposed CSI-free detector for SCW codes outperforms the baseline coherent and non-coherent detectors for uncoded transmission.

2.3 Challenges and Contributions

One of the main challenges of MC is to deal with the long tail of diffusive propagation that causes severe and peculiar inter-symbol-interference (ISI). One can increase the bit interval time to mitigate the ISI effect, but higher data rate justifies the optimization of the bit interval time to have few channel taps due to the ISI [57]. Even if one optimizes the bit interval time, the slow nature of diffusion makes the data rate still low. Using multiple-input multiple-output (MIMO) technique is a widely investigated solution to address this problem and can be adopted for MC [46, 47].

The main goal of this thesis is to propose a generalized and practical approach to design a Diffusive MIMO (D-MIMO) MC system based on block-type

communication where CIR is estimated at the beginning of each block and then it is used for equalization and detection for the rest of the block. D-MIMO molecular communication is an emerging area where recently has attracted some attentions. In [47], authors investigated various diversity techniques in D-MIMO communication assuming full knowledge of channel state information (CSI). The authors of [46], modeled the 2×2 D-MIMO channel by fitting a curve to the simulated data and proposed several detectors according the simulated channel response. Obtaining analytical solution of diffusive channel can be challenging. Even if we assume that solution is available, but the diffusion coefficient and transmitter-receiver distance is not known a priori and they are varying in time. Therefore, we need to estimate the CIR according to channel variation. We believe that knowledge of IR is so important for equalization and detection at the receiver.

This thesis introduce a matrix notation to model $M \times M$ D-MIMO systems and proposes a training-based MIMO channel estimation for $M \times M$ MC systems. In details, we extended the steps of R. Schober et. al. [35] to D-MIMO channel estimation by accounting for the inter-link diffusive-type interference. Furthermore, we propose a D-MIMO specific method for designing the training sequence that minimize the Cramér-Rao bound (CRB) at all receivers simultaneously.

In this thesis we adopt one-shot detectors for their low complexity. The proposed D-MIMO vector notation, let us introduce simple and efficient equalization and detection techniques. We have presented a threshold-based maximum likelihood detector. We have used blind equalizer (BE) and decision feedback equalizer (DFE) to mitigate the interference effect.BE is so simple but it is useful when interference is not severe. DFE is more complex and it has a good performance in the severe interference environment. Least Squares Detector (LSD) based on DFE is proposed which minimized the error probability. Generally, performance of the D-MIMO system is restricted by the inter-link interference (ILI). Therefore, MIMO time interleaving (TIL) modulation technique is introduced at transmitter site. It improves the performance of the system when transmit antennas are close to each other and ILI is severe.

Chapter 3

Diffusion Fundamentals

Diffusion is a well-known phenomena that exists in nature. There are many examples regarding diffusion such as change in the temperature of a room due to a sudden cold or hot source. The heat distributes according to the diffusion laws and the temperature reaches to equilibrium after required time. Likewise, cancer growth, angiogenesis and consequent invasion of the human body are diffusion processes too: tumoral cells are hungry of nutrients and oxygen and enter the competition with healthy tissue for space and energy [64, 65]. Additionally, in semiconductors the motion of electrons and relative holes follows diffusive process. At macroscopic level, the chaotic movement of charges generates an electron flux which moves in a continuous diffusive action, creating the diffusion current in electronic devices.

Diffusion process can be investigated through Fick's laws of diffusion. According to the Fick's first law, diffusive flux goes from region of high concentration, i.e., the transmitter, to the regions of low concentration, i.e., the receiver, with magnitude proportional to the concentration gradient. Fick's second law describes the motion of molecules with average molecules concentration $\bar{\rho}(x, y, z, t)$:

$$\frac{\partial \bar{\rho}(x, y, z, t)}{\partial t} = D\nabla^2 \bar{\rho}(x, y, z, t) \tag{3.1}$$

where diffusion coefficient D is given by Einstein relation [66]

$$D = \frac{K_B T}{6\pi\eta R_A} \tag{3.2}$$

where k_B is the Boltzman constant ($k_B = 1.38 \times 10^{-23}$), T is the temperature in kelvin, η is the viscosity of the medium in which the molecules are diffusing

and R_A is the molecule radius. Average molecules concentration $\bar{\rho}(x, y, z, t)$ is a function of space and time. After a specific long time we will reach to a steady state condition where the concentration all over the space is equal and the time derivative of the average concentration will be zero. This phenomena happens when you put some ink in a glass of water and the ink starts to diffuse till the ink concentration becomes equal in all the glass and we reach to the steady state situation.

Generally, deriving the close form solution of (3.1) is challenging. However, by considering some simplifying assumptions, such as, unbounded environment, point source, impulsive molecule release and transparent receivers [67, 68], we have:

$$\bar{\rho}(d, t) = \frac{N}{(4\pi D\, t)^{3/2}} \exp\Big(- \frac{d^2}{4D\, t} \Big) \tag{3.3}$$

where $\bar{\rho}(d, t)$ is the average local concentration molecule type A at receiver at time t after release of N molecules at $t = 0$ from transmitter, and d is the transmitter-receiver distance. We remark that Eqn.(3.3) gives the average local concentration of molecules of an ideal point source with an impulsive molecule release in an unbounded environment. In real settings, e.g. blood vessels, we confront a bounded environment where transmitter is not a point source that impulsively release molecules. Transmitter-receiver distance is not known a-priori and diffusion coefficient can not be simply calculated from (3.2). Situation would be much more complex when we consider all physical and chemical phenomenas that affect the channel between transmitter and receiver. We conclude the relation (3.3) is not valid in real settings and needs more careful treatment. However, it is useful to study the ideal case of diffusion as discussed above to gain insight about the diffusive channels. Studying diffusion channels help us understand the rules of the game and its comparison with EM channel help us to design more efficiently a diffusive MC system.

We define the channel impulse response (CIR) as the *expected* number of molecules at the receiver domain and at the time t denoted as $\bar{\boldsymbol{c}}(t)$ after instantaneous release of molecules at $t = 0$ [35], and it is given by the relation:

$$\bar{c}(d, t) = \iiint_V \bar{\rho}(d, t)\, dxdydz \tag{3.4}$$

We remark that $\bar{c}(t)$ is the expected number of molecules at receiver with volume V at time t due to the release of N molecules at $t = 0$ from transmitter. As shown in Fig. 3.1 the receiver is assumed to be a sphere with radius r_o.

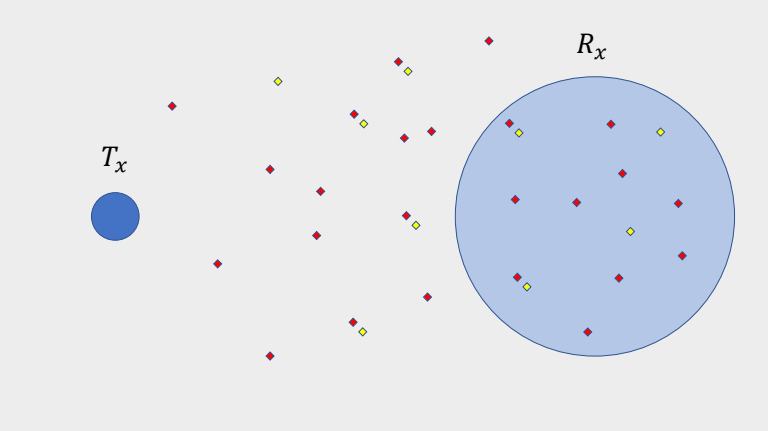

Figure 3.1: Topological model for a D-SISO MC system. The transmit antenna Tx release the same type of molecules (diamond shape), and molecules with yellow colors denoting to the interference molecules due to the previous transmissions

Average concentration of molecules can be approximated to be constant in the sphere if its size is small enough. Therefore, the Eqn. 3.3 and 3.4 can be written as

$$\bar{c}(d,t) = \frac{N \times V}{(4\pi D\, t)} \exp\Big(- \frac{d^2}{4D\, t} \Big)^{3/2} \tag{3.5}$$

where V is the volume of the sphere with radius r_o, N is the number of molecules released impulsively, d is the distance between transmitter and the receiver.

Fig. 3.1 shows the topological model of a D-SISO MC system where the system parameters are summarized in table 3.1. Fig.3.2 shows the CIR vs. time for the MC system with system parameters in Table 3.1. We highlight that the CIR is calculated according to Eqn. 3.5 for the ideal case of unbounded environment assuming a point source that impulsively release molecules. It can be observed that CIR is a pulse with one global maximum c_{max}, pulse delay τ_{max} and pulse width W which is shown in Fig. 3.2.

Diffusion is a stochastic phenomena and the number of observed molecules is a random value and is different with its mean value. Here, we assume the number of molecules at the receiver follows the Poisson distribution as introduced in [35, 34, 48] and the CIR is their mean number of molecules.

We remind that the CIR shown in Fig. 3.2 is obtained for an ideal environment. As explained before, for a bounded environment we can not use

Table 3.1: D-SISO system parameters used for CIR calculation

Parameter	Symbol	Value
N of molecules per emission	N	10^5
Symbol interval time	T_{int}	$0.2\,ms$
Diffusion coefficient	D	$10^{-9}\,\frac{m^2}{s}$
Transmitter-receiver distance	d	400 nm
Receiver radius	r_o	50 nm

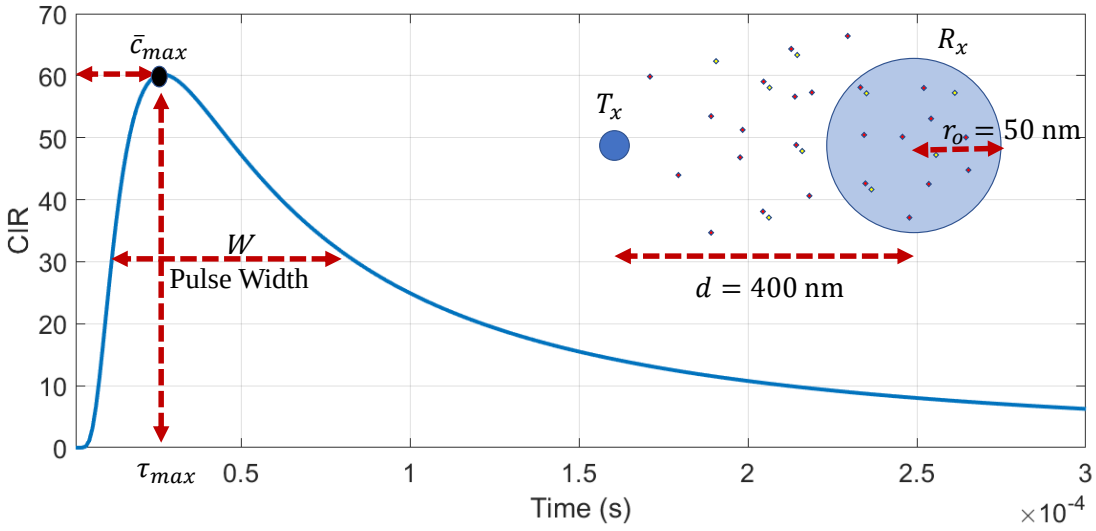

Figure 3.2: CIR vs. time for a D-SISO MC system with system parameters summarized in Table 3.1. Important channel parameters such as maximum amplitude $\bar{c}_{max}$, pulse delay τ_{max} and pulse width W are shown in the figure.

the above equations and it needs more careful treatment as we will discuss in details channel estimation in chapter 4. However, it is very important to understand the diffusion phenomena before we proceed to the channel estimation. In the following we discuss the most important channel parameters which help us to understand the diffusion phenomena and designing a diffusive MC system.

3.1 Pulse Delay

Propagation delay is defined as the elapsed time between the transmission and reception of the signal. We define the pulse delay τ_{max} as the time instant correspondent to the maximum received amplitude after instantaneous release of molecules. We have to find the time instant where CIR gets its global maximum st the receiver position. Since the $\bar{c}(t)$ is continuous we can find the global maximum by putting its derivative to zero.

$$\frac{\partial\, \bar{c}(d,t)}{\partial t} = \frac{\partial}{\partial t}\Big(\frac{N \times V}{(4\pi D\, t)^{3/2}} \exp\Big(- \frac{d^2}{4D\, t}\Big)\Big) = 0 \tag{3.6}$$

We find the propagation delay τ_{max}

$$\tau_{max} = \frac{d^2}{6\, D} \tag{3.7}$$

where d is the transmitter-receiver distance. It can be seen that the propagation delay is proportional to the square of distance and inverse of the diffusion coefficient as expected.

3.2 Pulse Amplitude

Pulse amplitude is defined as the maximum value of the received signal in time, at receiver position. Pulse amplitude is the amplitude of the $\bar{c}(t)$ at the time of the pulse delay:

$$\bar{c}_{max} = \bar{c}\,(d,t)\Big|_{t=\tau_{max}} = \Big(\frac{3}{2\pi e}\Big)^{3/2} \frac{N\, V}{d^3} \tag{3.8}$$

The pulse amplitude is an important parameter that indicate the expected number of molecules at the receiver domain after τ_{max} of releasing molecules.

We remind that the number of observed molecules at τ_{max} is a Poisson random variable with parameter $\bar{c}_{max}$. We note that the pulse amplitude is independent of diffusion coefficient D. It means that even if you change the medium with different diffusivity, still the pulse amplitude does not change when transmitter-receiver distance d does not change. Diffusivity only change the speed of diffusion and τ_{max} but not the amplitude. The pulse amplitude inversely is proportional to the cube of transmitter-receiver distance d.

3.3 Pulse Width

As it is usually done in electromagnetic communications, we compute the pulse width at the 50% level, i.e., the time interval at which the pulse has an amplitude greater than half of its maximum value:

$$\bar{c}(d,t) = \frac{\bar{c}_{max}}{2} = \frac{1}{2}(\frac{3}{2\pi e})^{3/2}\,\frac{N\,V}{d^3} \tag{3.9}$$

This equation has two solutions, corresponding to the two time instants at which the pulse amplitude is equal to half of its maximum value. These instants are given by [69]:

$$t_1 = \frac{0.0728}{D}\,d^2 \qquad t_2 = \frac{0.5229}{D}\,d^2 \tag{3.10}$$

Finally, we can obtain the expression of the pulse width W by subtracting these two instants:

$$W = t_2 - t_1 = \frac{0.4501}{D}\,d^2 \tag{3.11}$$

It can be observed that the pulse width W is inversely proportional to the diffusion coefficient and it is proportional to the square of transmitter-receiver distance d. Therefore, a medium with high diffusivity will leads to a narrower pulse width that decreases the interference.

3.4 Molecular vs Electromagnetic channel

Diffusive channel exhibits unique features which makes it different from conventional electromagnetic channel. Therefore, an in-depth study is needed to gain insight of diffusive channel over the well-known EM channel to understand their difference and performances.

In diffusive channel pulse delay is proportional to the square of transmission distance $\tau_{max} \propto d^2$ while in EM channel it increases linearly with propagation

Table 3.2: Diffusive channel vs. Electromagnetic channel

Feature	EM Channel	Diffusive Channel
Channel Type	Definitive	Stochastic
Propagation Speed	$c = 3 \times 10^8$ m/s	$\propto \frac{1}{d}$
Propagation Range	$10^3 - 10^5$ m	$10^{-8} - 10^{-5}$ m
Pulse Delay	$\propto d$	$\propto d^2$
Pathloss	$\propto \frac{1}{d}$	$\propto \frac{1}{d^3}$
Pulse Width	$\propto 1$	$\propto d^2$

distance. Pulse amplitude in diffusive channel is proportional to $\bar{c}_{max} \propto \frac{1}{d^3}$ while in EM channel in free space, the pathloss is proportional to $\propto \frac{1}{d}$. So, the range of communication in diffusive channels is so small and it is limited to few micrometers. Pulse width W which is an indication of distortion is proportional with $\propto d^2$ in diffusive channel while in free space EM propagation, distortion is negligible. Finally, we remind that the diffusive channel is stochastic while EM channel is definitive. It means that even if we assume CIR is known and there is no noise and interference, the observed number of molecules is a random variable that approximately it follows the Poisson distribution with the parameter CIR. Therefore, we can say there is an intrinsic noise, e.g. like the shot noise in photon counting process, which the variance of the noise is proportional to the $\propto \bar{c}$. Table 3.2 summarizes all the above discussion concisely.

Chapter 4

System Model

4.1 Single-Input Single-Output (SISO)

We consider a single-transmitter single-receiver diffusive MC system as shown in Fig. 3.1. We assume ON-OFF key signaling means that at the beginning of each bit interval time, the transmitter release N information molecules. Receiver is assumed to be synchronized with the transmitter such that it counts the molecules at the time where number of observed molecules expected to be maximum.

Diffusive channel has a long memory such that the receiver counts molecules from previous bit interval times and it is known as inter-symbol interference (ISI). One can mitigate the effect of the ISI by making the bit interval time so long. Considering the ISI, we can obtain the observed number of molecules at $k-th$ time interval $y[k]$ with the following equation

$$y[k] = \sum_{\ell=0}^{L-1} c[\ell, k]x[k-\ell] + v[k] \tag{4.1}$$

where $c[\ell, k]$ is a random variable and denotes to the observed number of molecules detected at time $k-\ell$ when the transmitter release $x[k]\times N$ molecules at the beginning of that time interval and x is the binary information. L is the number of channel memory taps and it depends on system configuration and bit interval time. $c[\ell, k]$ is a random variable and it follows Poisson distribution with the mean $\bar{c}[\ell]$: $c[\ell, k] \sim Poiss\left(\bar{c}[\ell]\right)$. $v[k]$ is the number of noise molecules which is a random variable and it similarly follows Poisson distribution: $v[k] \sim Poiss\left(\bar{v}\right)$ [34, 35]. Therefore, the expected number of molecules to be detected

at $k-th$ time interval is [35, 48].

$$\bar{y}[k] = \mathbb{E}\left\{y[k]\right\} = \sum_{\ell=0}^{L-1} \bar{c}[\ell] x_i[k-\ell] + \bar{v}. \tag{4.2}$$

We can write the Eqn. (4.2) compactly as follows:

$$\bar{y}[k] = \boldsymbol{x}^T[k]\, \bar{\boldsymbol{c}} \tag{4.3}$$

where $\bar{\boldsymbol{c}} = [\bar{c}[0], \bar{c}[1], ..., \bar{c}[L-1], \bar{v}]^T$ is a $(L+1) \times 1$ vector containing the CIR vector in terms of mean of the Poisson distribution and noise, $\boldsymbol{x}[k] = [x[k], x[k-1], ..., x[k-\ell+1], 1]^T$ is a $(L+1) \times 1$ vector denoting current time and $L-1$ previous transmitted bits and the last entry is always 1 due to the existence of noise.

4.2 Multiple-Input Multiple-Output (MIMO)

We consider a $M \times M$ D-MIMO system for MC as shown in Fig. 4.1. The system consists of M pair of transmitters denoted as Tx_i, and receivers Rx_j, where $i, j \in \{1, 2, 3...M\}$. We assume that all transmitters emit the same type of molecules. Each transmitter emits a known number of molecules N at the beginning of each symbol intervals. The molecules diffuse in the environment and some of them reach the M receivers. Transmitters and receivers are not fixed in their position and could slightly move on fluid where molecules diffuse, so the CIR changes over time.

Transmitters modulate the molecules density using concentration shift keying (CSK) and the receivers count the number of molecules at the time of sampling. As customary, we set the sampling time so that the number of molecules at receivers for the corresponding transmitters is maximized. As shown in Fig. 4.2, the channel has memory and due to the inter-symbol-interference (ISI), the receiver counts the molecules from previous samples of the corresponding transmitter. Similarly, the molecules from the current and previous samples of the non-corresponding transmitters are known as inter-link-interference (ILI). L is the number of channel taps for each link that is related to the system geometry, configuration and bit interval time. Specifically, we can eliminate the ISI and ILI by making the bit interval time large enough and putting each pair of transceivers far enough from the other pairs. However, this case is not considered due to the demands for high data rate per unit of space. Hence,

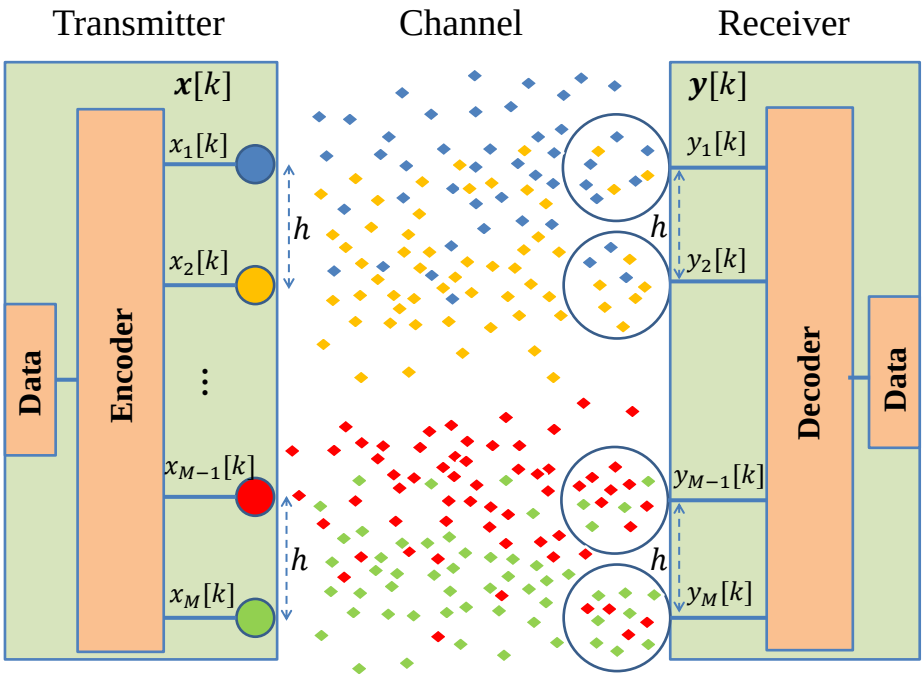

Figure 4.1: Topological model for $M \times M$ D-MIMO system. The M transmit antennas $(Tx_1, ..., Tx_M)$ release the same type of molecules (diamond shape), and molecules here have different colors according to the corresponding transmitter to visualize the interference phenomena

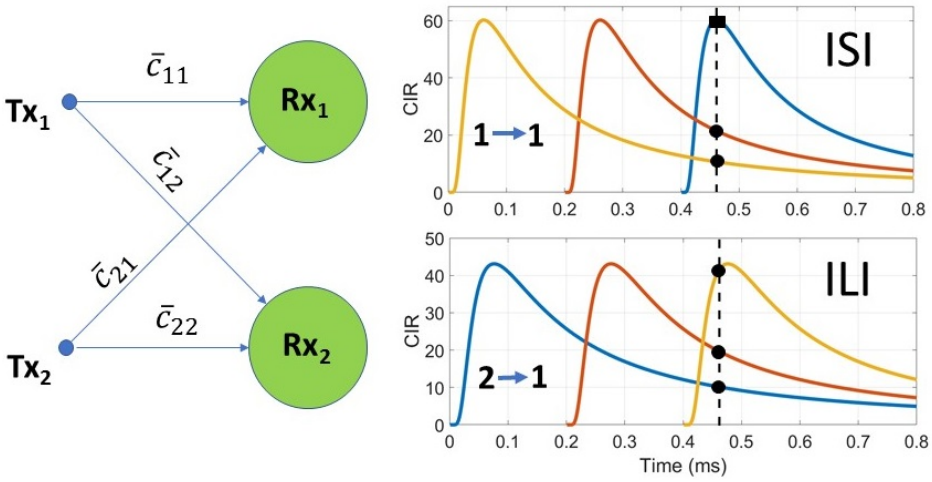

Figure 4.2: Impulse response, $\bar{c}_{ij}(t)$, of a 2×2 D-MIMO system at Rx_1 vs time, for 3 emissions of molecules with time spacing $0.2\,ms$: ILI and ISI are black dots.

we have to face the ISI and ILI in the MC system and try to mitigate their effects. The observed number of molecules at sampling time k and receiver j is

$$y_j[k] = \sum_{i=1}^{M} \sum_{\ell=0}^{L-1} c_{ij}[\ell, k] x_i[k-\ell] + v_j[k] \tag{4.4}$$

where $c_{ij}[\ell, k]$ is a random variable that denotes to the number of molecules observed at time k by the receive antenna Rx_j from transmit antenna Tx_i due to the release of N molecules at the time $[k-\ell]$. Case $i = j$ refers to the paired transmitter-receiver, otherwise it refers to the inter-link interference. $x_i[k] \in \{0, 1\}$ is the transmitted symbol at the time interval k from transmit antenna Tx_i. The number of molecules $c_{ij}[\ell, k]$ can be approximated as a Poisson random variable with a mean value $\bar{c}_{ij}[\ell]$: $c_{ij}[\ell, k] \sim Poiss\,(\bar{c}_{ij}[\ell])$. Additionally, $v_j[k]$ is the number of external noise molecules detected at the receiver j at time interval k. Noise molecules could originate from the remaining channel taps from all transmitters not considered in model, and any external source. Hence, we can consider the noise as a Poisson with a mean $\bar{v}_j$: $v_j[k] \sim Poiss\,(\bar{v}_j)$ [34, 35].

Assume that $\boldsymbol{x}[k] = [x_1[k], x_2[k], ..., x_M[k]]^T$ is a binary data at time interval k at all M transmitters. To avoid edge effect due to the ISI, we employ $y_j[k]$

for $k \geq L$. The expected number of molecules at $k-th$ time interval and $j-th$ receiver is:

$$\bar{y}_j[k] = \mathbb{E}\left\{y_j[k]\right\} = \sum_{i=1}^{M}\sum_{\ell=0}^{L-1} \bar{c}_{ij}[\ell]x_i[k-\ell] + \bar{v}_j \tag{4.5}$$

where $L \leq k \leq K$. Eqn. (4.5) can be written compactly as:

$$\bar{y}_j[k] = \boldsymbol{X}^T[k]\bar{\boldsymbol{C}}_j \tag{4.6}$$

where the following notations are used:

$$\boldsymbol{X}[k] = [\boldsymbol{x}^T[k], \boldsymbol{x}^T[k-1], ..., \boldsymbol{x}^T[k-L+1], 1]^T$$

$$\bar{\boldsymbol{c}}_j[\ell] = [\bar{c}_{1j}[\ell], \bar{c}_{2j}[\ell], ..., \bar{c}_{Mj}[\ell]]^T$$
$$\bar{\boldsymbol{C}}_j = [\bar{\boldsymbol{c}}_j^T[0], \bar{\boldsymbol{c}}_j^T[1], ..., \bar{\boldsymbol{c}}_j^T[L-1], \bar{v}_j]^T$$

here, $\bar{\boldsymbol{c}}_j[\ell]$ is a vector with dimension $M \times 1$ containing the information of the expected number molecules at receiver j form the $\ell - th$ previous molecule release of all transmit antennas, and $\boldsymbol{x}[k-\ell]$ is its corresponding transmitted vector. Additionally, $\bar{\boldsymbol{C}}_j$ is a $(ML+1)\times 1$ vector collecting all channel memory taps of receiver j from all transmit antennas and noise $\bar{v}_j$. $\boldsymbol{X}[k]$ with dimension $(ML+1)\times 1$ collects training sequence vectors of current and $\ell - th$ previous time intervals.

The expected number of molecules at receiver j during the time intervals $L \leq k \leq K$ is defined as $\bar{\boldsymbol{y}}_j = [\bar{y}_j[L], \bar{y}_j[L+1]..., \bar{y}_j[K]]^T$, and the D-MIMO relation for receiver j is written

$$\underset{(K-L+1)\times 1}{\bar{\boldsymbol{y}}_j} = \underset{(K-L+1)\times(ML+1)}{\boldsymbol{X}^T} \underset{(ML+1)\times 1}{\bar{\boldsymbol{C}}_j} \tag{4.7}$$

$$\begin{bmatrix} \bar{y}_j[L] \\ \bar{y}_j[L+1] \\ \vdots \\ \bar{y}_j[K] \end{bmatrix} = \begin{bmatrix} \boldsymbol{x}[L] & \boldsymbol{x}[L+1] & \dots & \boldsymbol{x}[K] \\ \boldsymbol{x}[L-1] & \boldsymbol{x}[L] & \dots & \boldsymbol{x}[K-1] \\ \vdots & \vdots & \ddots & \vdots \\ \boldsymbol{x}[1] & \boldsymbol{x}[2] & \dots & \boldsymbol{x}[K-L+1] \\ 1 & 1 & \dots & 1 \end{bmatrix}^T \begin{bmatrix} \bar{\boldsymbol{c}}_j[0] \\ \bar{\boldsymbol{c}}_j[1] \\ \vdots \\ \bar{\boldsymbol{c}}_j[L-1] \\ \bar{v}_j \end{bmatrix}$$

where $\boldsymbol{X}$ is a $(ML+1)\times(K-L+1)$ convolution matrix of training sequences including memory of previous samples due to the channel taps, and it is defined as

$$\boldsymbol{X} = [\boldsymbol{X}[L], \boldsymbol{X}[L+1], ..., \boldsymbol{X}[K]] \tag{4.8}$$

Finally, we define $\bar{\boldsymbol{Y}} = [\bar{\boldsymbol{y}}_1, \bar{\boldsymbol{y}}_2 ..., \bar{\boldsymbol{y}}_M]$ and we compactly write the global D-MIMO relation into

$$\underset{(K-L+1)\times(M)}{\bar{\boldsymbol{Y}}} = \underset{(K-L+1)\times(ML+1)}{\boldsymbol{X}^T} \quad \underset{(ML+1)\times M}{\bar{\boldsymbol{C}}} \tag{4.9}$$

$$\begin{bmatrix} \bar{y}_1[L] & \bar{y}_2[L] & \dots & \bar{y}_M[L] \\ \bar{y}_1[L+1] & \bar{y}_2[L+1] & \dots & \bar{y}_M[L+1] \\ \vdots & \vdots & \ddots & \vdots \\ \bar{y}_1[K] & \bar{y}_2[K] & \dots & \bar{y}_M[K] \end{bmatrix} =$$

$$\begin{bmatrix} \boldsymbol{x}[L] & \boldsymbol{x}[L+1] & \dots & \boldsymbol{x}[K] \\ \boldsymbol{x}[L-1] & \boldsymbol{x}[L] & \dots & \boldsymbol{x}[K-1] \\ \vdots & \vdots & \ddots & \vdots \\ \boldsymbol{x}[1] & \boldsymbol{x}[2] & \dots & \boldsymbol{x}[K-L+1] \\ 1 & 1 & \dots & 1 \end{bmatrix}^T \begin{bmatrix} \bar{\boldsymbol{c}}_1[0] & \bar{\boldsymbol{c}}_2[0] & \dots & \bar{\boldsymbol{c}}_M[0] \\ \bar{\boldsymbol{c}}_1[1] & \bar{\boldsymbol{c}}_2[1] & \dots & \bar{\boldsymbol{c}}_M[1] \\ \vdots & \vdots & \ddots & \vdots \\ \bar{\boldsymbol{c}}_1[L-1] & \bar{\boldsymbol{c}}_2[L-1] & \dots & \bar{\boldsymbol{c}}_M[L-1] \\ \bar{v}_1 & \bar{v}_2 & \dots & \bar{v}_M \end{bmatrix}$$

where $\bar{\boldsymbol{C}}$ is the $(ML+1)\times M$ global channel matrix, and it is defined as

The matrix of all the observed number of molecules at the M receivers contain the Poisson random variables with mean equal to $\bar{\boldsymbol{Y}}$:

$$\boldsymbol{Y} = Poiss\,(\bar{\boldsymbol{Y}}) \tag{4.10}$$

which means each entry of the observed matrix $\boldsymbol{Y}$, is Poisson random variable with mean equal to the corresponding entry of $\bar{\boldsymbol{Y}}$.

To better understand the D-MIMO model, assume a 2×2 D-MIMO system configuration in Fig. 4.2 with $L = 3$ channel taps and time interval $0 < k \leq K$ where $K = 6$. Then we have

$$\begin{bmatrix} \bar{y}_1[3] & \bar{y}_2[3] \\ \bar{y}_1[4] & \bar{y}_2[4] \\ \bar{y}_1[5] & \bar{y}_2[5] \\ \bar{y}_1[6] & \bar{y}_2[6] \end{bmatrix} = \begin{bmatrix} x_1[3] & x_1[4] & x_1[5] & x_1[6] \\ x_2[3] & x_2[4] & x_2[5] & x_2[6] \\ x_1[2] & x_1[3] & x_1[4] & x_1[5] \\ x_2[2] & x_2[3] & x_2[4] & x_2[5] \\ x_1[1] & x_1[2] & x_1[3] & x_1[4] \\ x_2[1] & x_2[2] & x_2[3] & x_2[4] \\ 1 & 1 & 1 & 1 \end{bmatrix}^T \begin{bmatrix} \bar{c}_{11}[0] & \bar{c}_{12}[0] \\ \bar{c}_{21}[0] & \bar{c}_{22}[0] \\ \bar{c}_{11}[1] & \bar{c}_{12}[1] \\ \bar{c}_{21}[1] & \bar{c}_{22}[1] \\ \bar{c}_{11}[2] & \bar{c}_{12}[2] \\ \bar{c}_{21}[2] & \bar{c}_{22}[2] \\ \bar{v}_1 & \bar{v}_2 \end{bmatrix}$$

Chapter 5

D-MIMO Channel Estimation

Diffusive channel is highly complex. Previously we have shown the solution of diffusion equation (3.1) in an ideal environment. The solution is valid only for an unbounded environment with an impulsive molecule release and static diffusive channel. It is assumed that we know a-priori the transmitter-receiver distance, diffusion coefficient and other system parameters. However, we are dealing with real environments where it is bounded and we do not know system parameters a-priori. Additionally, transmitter is not able to impulsively release molecules. Moreover, diffusive channel is not static and channel varies during the time. CIR is highly dependent on transmitter-receiver distance. In environments where there is flows, e.g. blood vessels, CIR changes rapidly. There are other physical and chemical phenomenas that makes the diffusion channel more complex such as molecules degradation, recombination, enzymes and etc.

We believe that CIR can not be accurately calculated off-line according to the diffusion laws because of the highly complex diffusion environment. Channel estimation is the only way that relieve us from considering all physical and chemical phenomenas. We assume that channel remains unchanged during the channel coherence time T_c. Channel coherence time depends on the environment and system configuration; for example in blood vessels where there is a constant flow channel coherence time is small. We assume block-type communication and the block length B depends on the channel coherence time T_c and bit interval time T_{int}. According to the potential application and working environment, we can estimate channel coherence time and choose the optimal block length. At the beginning of each block, transmitter sends a designed training sequence and receiver estimate the CIR by knowing what is transmitted and

what it is detected. The estimated CIR then can be used for equalization and detection for the rest of that block.

5.1 Problem Definition

Assume that $\boldsymbol{s}_i = [s_i[1], s_i[2], ..., s_i[K]]^T$ is a binary training sequence with length K for transmitter i. To avoid edge effect due to the ISI, in CIR estimation we employ $y_j[k]$ for $k \geq L$. Therefore, the $K - L + 1$ samples are used for CIR estimation of the j-th receiver. As previously explained we use the following notations for the training sequence:

$$\boldsymbol{s}[k] = [s_1[k], s_2[k], ..., s_M[k]]^T$$

$$\boldsymbol{S}[k] = [\boldsymbol{s}^T[k], \boldsymbol{s}^T[k-1], ..., \boldsymbol{s}^T[k-L+1], 1]^T$$

The probability density function (PDF) of all observations at all receivers are the product of the Poisson distribution of each observation at each receiver

$$f_{\boldsymbol{Y}}\left(\boldsymbol{Y}|\bar{\boldsymbol{C}}, \boldsymbol{S}\right) = \prod_{k=L}^{K} \prod_{j=1}^{M} \frac{\left(\boldsymbol{S}^T[k]\bar{\boldsymbol{C}}_j\right)^{y_j[k]} \exp(-\boldsymbol{S}^T[k]\bar{\boldsymbol{C}}_j)}{y_j[k]\,!} \tag{5.1}$$

According to (4.7), we can analyze the performance of each receiver independently to make sure that all M receivers are simultaneously working optimally. Therefore, the PDF of the observations of j-th receiver is

$$f_{\boldsymbol{y}_j}\left(\boldsymbol{y}_j|\bar{\boldsymbol{C}}_j, \boldsymbol{S}\right) = \prod_{k=L}^{K} \frac{\left(\boldsymbol{S}^T[k]\bar{\boldsymbol{C}}_j\right)^{y_j[k]} \exp(-\boldsymbol{S}^T[k]\bar{\boldsymbol{C}}_j)}{y_j[k]\,!}, \tag{5.2}$$

The goal is to estimate the CIR by knowing the training sequence considering the likelihood function above.

5.2 Cramér-Rao Bound

The Cramér-Rao bound (CRB) sets the lower bound on the covariance of any unbiased estimator of a deterministic parameters. Let $\hat{\bar{\boldsymbol{C}}}_j$ be the unbiased estimator of $\bar{\boldsymbol{C}}_j$, the CRB sets the bound of the covariance

$$cov(\hat{\bar{\boldsymbol{C}}}_j) \succeq \boldsymbol{I}^{-1}(\bar{\boldsymbol{C}}_j) \tag{5.3}$$

where $\boldsymbol{I}(\bar{\boldsymbol{C}}_j)$ is the Fisher information matrix of $\bar{\boldsymbol{C}}_j$ and is given by

$$\boldsymbol{I}(\bar{\boldsymbol{C}}_j) = \mathbb{E}_{\boldsymbol{y}_j}\{-\frac{\partial\ \mathcal{L}_{\boldsymbol{y}_j}\left(\boldsymbol{y}_j|\bar{\boldsymbol{C}}_j, \boldsymbol{S}\right)}{\partial\bar{\boldsymbol{C}}_j\partial\bar{\boldsymbol{C}}_j}\}, \tag{5.4}$$

Therefore, the CRB of the receiver j is given by

$$CRB_j = tr\{\boldsymbol{I}^{-1}(\bar{\boldsymbol{C}}_j)\} = tr\left\{\left[\sum_{k=L}^{K}\frac{\boldsymbol{S}[k]\boldsymbol{S}^T[k]}{\boldsymbol{S}^T[k]\bar{\boldsymbol{C}}_j}\right]^{-1}\right\}. \tag{5.5}$$

and this sets the reference bound at each receive antenna.

5.3 Maximum Likelihood CIR estimator

Maximum likelihood (ML) D-MIMO CIR estimator finds the positive values of $\bar{\boldsymbol{C}}_j$ which maximize the likelihood of the observation vector $\boldsymbol{y}_j$

$$\begin{aligned}\hat{\bar{\boldsymbol{C}}}_j^{\mathrm{ML}} &= \underset{\bar{\boldsymbol{C}}_j\geq 0}{\operatorname{argmax}}\ f_{\boldsymbol{y}_j}\left(\boldsymbol{y}_j|\bar{\boldsymbol{C}}_j, \boldsymbol{S}\right)\\ &= \underset{\bar{\boldsymbol{C}}_j\geq 0}{\operatorname{argmax}}\ \mathcal{L}_{\boldsymbol{y}_j}\left(\boldsymbol{y}_j|\bar{\boldsymbol{C}}_j, \boldsymbol{S}\right)\end{aligned} \tag{5.6}$$

where the log likelihood function is

$$\mathcal{L}_{\boldsymbol{y}_j}\left(\boldsymbol{y}_j|\bar{\boldsymbol{C}}_j, \boldsymbol{S}\right) = \sum_{k=L}^{K}\left[-\boldsymbol{S}^T[k]\bar{\boldsymbol{C}}_j + y_j[k]\ln(\boldsymbol{S}^T[k]\bar{\boldsymbol{C}}_j)\right] \tag{5.7}$$

Maximizing the log likelihood function is a convex optimization problem. $\ln(.)$ is a strictly concave function and $(\boldsymbol{S}^T[k]\bar{\boldsymbol{C}}_j)$ is affine. So, $\ln(\boldsymbol{S}^T[k]\bar{\boldsymbol{C}}_j)$ is strictly concave. Therefore, the $\mathcal{L}$ is weighted sum of concave terms and the maximum of a concave function is given by setting its derivative respect to the $\bar{\boldsymbol{C}}_j$ to zero [35].

The ML estimate of the CIR for the D-MIMO channel at receiver j is obtained by solving a system of non-linear equations given below [35]:

$$\sum_{k=L}^{K}\left[\frac{y_j[k]\boldsymbol{S}[k]}{\boldsymbol{S}^T[k]\bar{\boldsymbol{C}}_j} - \boldsymbol{S}[k]\right] = \boldsymbol{0} \tag{5.8}$$

We note entries of $\bar{\boldsymbol{C}}_j$ are positive semidefinite. However, ML estimator could estimate a negative value for some elements of the $\bar{\boldsymbol{C}}_j$. Sub-optimal solution is to set to zero all the negative entries of the estimated CIR. This heuristic approach was adopted for single link MC [35], and showed therein a negligible loss of performances compared to the optimal ML. Therefore, sub-optimal solution of (5.8) is highly preferred in D-MIMO channels due to its simplicity.

5.4 Least Squares CIR Estimator

The Least-Squares (LS) method chooses $\bar{\boldsymbol{C}}$ which minimizes the sum of the square errors at all receiver from the observation vector $\boldsymbol{Y}$,

$$\hat{\bar{\boldsymbol{C}}}^{LS} = \underset{\bar{\boldsymbol{C}} \geq 0}{\operatorname{argmin}} \ \|\boldsymbol{\epsilon}\|^2. \tag{5.9}$$

where $\boldsymbol{\epsilon} = \boldsymbol{Y} - \mathbb{E}\{\boldsymbol{Y}\} = \boldsymbol{Y} - \boldsymbol{S}^T\bar{\boldsymbol{C}}$. The square norm of the error is given as

$$\begin{aligned} \|\boldsymbol{\epsilon}\|^2 &= tr\{\boldsymbol{\epsilon}\boldsymbol{\epsilon}^T\} = tr\{(\boldsymbol{Y} - \boldsymbol{S}^T\bar{\boldsymbol{C}})(\boldsymbol{Y} - \boldsymbol{S}^T\bar{\boldsymbol{C}})^T\} \\ &= tr\{\boldsymbol{S}\boldsymbol{S}^T\bar{\boldsymbol{C}}\bar{\boldsymbol{C}}^T\} - 2tr\{\boldsymbol{Y}^T\boldsymbol{S}^T\bar{\boldsymbol{C}}\} + tr\{\boldsymbol{Y}\boldsymbol{Y}^T\} \end{aligned} \tag{5.10}$$

The square norm of the error matrix, $\|\boldsymbol{\epsilon}\|^2$ is a convex function because it is a quadratic form in $\bar{\boldsymbol{C}}$ and $\boldsymbol{S}\,\boldsymbol{S}^T \geq 0$. Hence, to minimize the function we put its first derivative respect to $\boldsymbol{C}$ to the zero.

$$\frac{\partial\|\boldsymbol{\epsilon}\|^2}{\partial\bar{\boldsymbol{C}}} = 2\boldsymbol{S}\,\boldsymbol{S}^T\boldsymbol{C} - 2\boldsymbol{S}\boldsymbol{Y} = 0. \tag{5.11}$$

Finally, the LS estimate of the CIR for D-MIMO channel is

$$\hat{\bar{\boldsymbol{C}}}^{LS} = \Big[(\boldsymbol{S}\,\boldsymbol{S}^T)^{-1}\,\boldsymbol{S}\,\boldsymbol{Y}\Big]. \tag{5.12}$$

Minimization of (5.9) is a constrained optimization problem with $\boldsymbol{C} \geq 0$ for entries. In case there exist a stationary point, this is the global optimum solution. In case the stationary point does not exist, sub-optimal solution is to set all negative elements of $\boldsymbol{C}$ to zero. Optimal solution for (5.9) is introduced in [35], and the authors showed that for K large, there exist a stationary point, and for small lengths, the performance loss is very negligible. Again, we prefer the sub-optimal solution for D-MIMO system due to its simplicity.

5.5 Training Sequence Design

In this section, we present a method for designing the training sequences for estimating the CIR of a D-MIMO channel. As shown in (5.5), the CRB for a given system is a function of training sequences. Therefore, we can find a set of training sequences that minimize the CRB of all receivers. In other words, the CRB of a specific receiver depends on the training sequence of all transmitters which have interference with it. In general, for a $M \times M$ D-MIMO system, we have to design M different training sequences to minimize the CRB of all receivers simultaneously. However, in practice we do not need to design M training sequences, because ILI for far transmitters is negligible and thus we neglect their interference channels but consider them as an augmented noise source in v_j. In order to find a suitable set of training sequences that simultaneously minimize all CRBs, we consider following constraints: 1) the training sequences should be molecularly efficient by minimizing the fraction of molecules used for channel estimation, and 2) transmitters can not be silent for many consequent intervals. In detail, for a training sequence of length K, we consider sequences with maximum $K/2$ ones, consequently transmitting maximum $NK/2$ molecules, and the maximum consequent zeros are considered 4 time intervals. $\mathcal{S}$ is the sets of all possible training sequences that meet the above criteria.

$$[\boldsymbol{s}_1, \boldsymbol{s}_2, ..., \boldsymbol{s}_M] = \underset{\boldsymbol{s}_i \in \mathcal{S}}{\operatorname{argmin}} \{CRB_1, \dots CRB_M\} \tag{5.13}$$

Accuracy of CIR estimation depends on the training sequence length, hence K should chosen carefully. For large K, it is difficult to search among all suitable sets to find the optimum ones. Therefore, we look for an optimum training sequence with smaller length $K_1 << K$, that is concatenated to build a longer training sequence of length K. provided that K_1 is wisely selected, concatenating would not impair the performances.

5.6 Channel Estimation Performance Analysis

In this section, we present a 2×2 D-MIMO configuration and we compare the performances of the channel estimators introduced in this chapter for ON-OFF keying signaling. We have generated the CIR according to the analytical models proposed in [26, 54] for MC systems. However, there is no constraint in the value of CIR to be estimated. Diffusion coefficient value is $10^{-9} m^2/s$ and

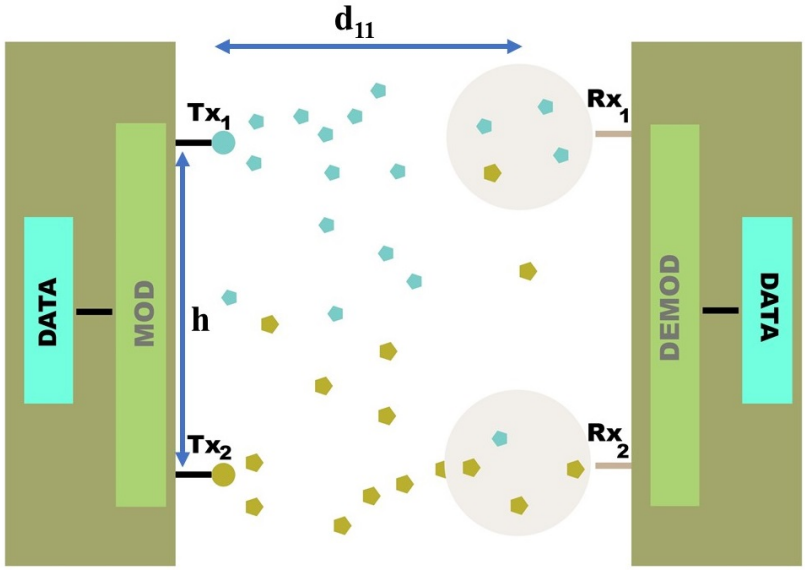

Figure 5.1: Topological model for a 2×2 MC-MIMO system. Both transmitter use the same information molecule (pentagon). Molecules colors correspond to their transmitter color. .

it is compatible to the normal values of diffusion of most of molecules in water at room temperature. Choosing bit interval time is a trade-off between bit rate and total number LM of ISI and ILI of the channel memory to be estimated. Bit interval time is $T_{int} = 0.2\,ms$, all transmitters release $N = 10^5$ molecules and the receivers counts once the number of molecules per each symbol at time which CIR of the pair transmitter is expected to be maximum. For simplicity, the mean of noise is chosen as $\bar{v}_j = 0.3\,\bar{c}_{jj}(0)$. The number of channel taps for both ISI and ILI link are considered $L = 3$, so $\bar{c}_{ij}[L] \leq 0.05\,\bar{c}_{jj}[0]$.

The 2×2 D-MIMO system is shown in Fig. (5.1). We have assumed that the distance between transmitter and receiver is $d = 400\,nm$ and the inter-distance is $h = 200\,nm$. Spherical receiver with radius $20\,nm$ is assumed. Positions of the mentioned entities are fluctuating: $P_{Tx_1} = (0+\delta x_1, 0+\delta y_1, 0+\delta z_1), P_{Tx_2} = (0+\delta x_2, h+\delta y_2, 0+\delta z_2), P_{Rx_1} = (d+\delta x_3, 0+\delta y_3, 0+\delta z_3), P_{Rx_2} = (d+\delta x_4, h+\delta y_4, 0+\delta z_4)$, with $\delta_{x,y,z} \sim \mathcal{N}(0, \sigma^2)$, and $\sigma^2 = 50\,nm$. Since the Tx and Rx are not fixed in the position, the channel is varying in time. While the entities are fixed, the CIR at the receivers are:

$$\bar{\boldsymbol{C}}_1 = [60.21, 41.58, 9.11, 8.71, 3.83, 3.74, 18.06]^T$$

$$\bar{\boldsymbol{C}}_2 = [41.58, 60.21, 8.71, 9.11, 3.74, 3.83, 18.06]^T.$$

We note that in each realization the CIR is different, $\bar{\boldsymbol{C}}_1 \neq \bar{\boldsymbol{C}}_2$, because the position of transmitters and receivers are changing with normal distribution with $\sigma^2 = 20\,nm$. The training sequences are designed according to (5.13) with the length $K_1 = 16$ and they are

$$\boldsymbol{s}_1 = [1, 1, 1, 0, 0, 0, 0, 1, 0, 1, 0, 1, 1, 0, 0, 1]^T$$

$$\boldsymbol{s}_2 = [1, 1, 1, 0, 1, 0, 0, 0, 1, 1, 1, 0, 0, 0, 0, 1]^T.$$

Longer training sequences are constructed by concatenating these training sequences as detailed in subsection 3.5.

In this problem, each receiver has to estimate $LM + 1 = 7$ variables, for a total of 14 variables. The results in Fig. 5.2, are Monte Carlo simulations with 1000 random CIR realizations.

Fig. 5.2 shows the performance of the system in terms of mean square error (MSE), $\mathbb{E}\left\{||\hat{\bar{\boldsymbol{c}}}_j - \bar{\boldsymbol{c}}_j||^2\right\}$ in dB vs. the training sequence length (K) for the ML and LS estimators. The MSE decreases with increasing the training sequence length as we expected. We can notice that training sequences are designed such that both receivers have optimum performances for both estimators as they attain the corresponding CRB. Fig. 5.3, shows the Normalized MSE which is defined by

$$MSE_j^N = \frac{\mathbb{E}\left\{||\hat{\bar{\boldsymbol{c}}}_j - \bar{\boldsymbol{c}}_j||^2\right\}}{||\mathbb{E}\{\bar{\boldsymbol{c}}_j\}||^2}. \tag{5.14}$$

The value of the normalized MSE is much lower, around 38dB, than the MSE. As we can see in Fig. 5.3, the performance of the ML estimator outperforms the LS estimator by approximately 1 dB. However, the LS estimator is preferred due to its simplicity respect to the ML estimator, because our bio-based receivers have limited computational capabilities. In applications where receivers send the data to the external computers, the ML estimator is preferred because it reaches to the CRB bound.

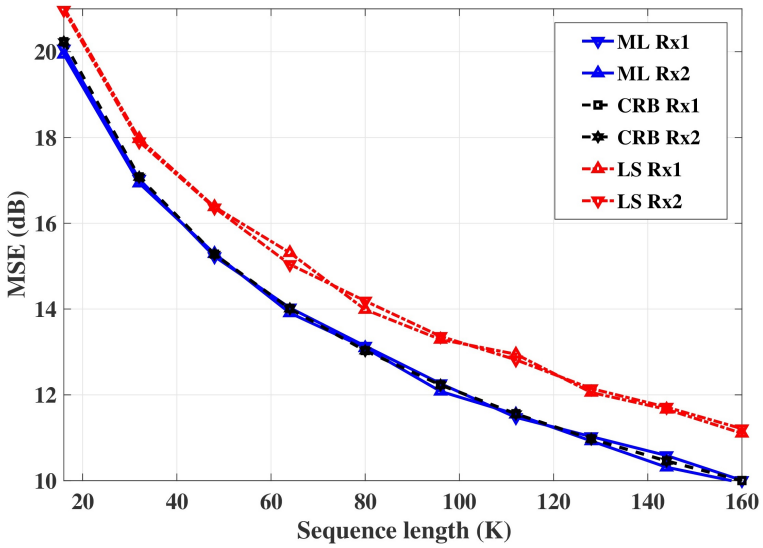

Figure 5.2: Channel estimators: ML, LS and CRB vs. the training sequence length K for a 2×2 D-MIMO system and $L = 3$.

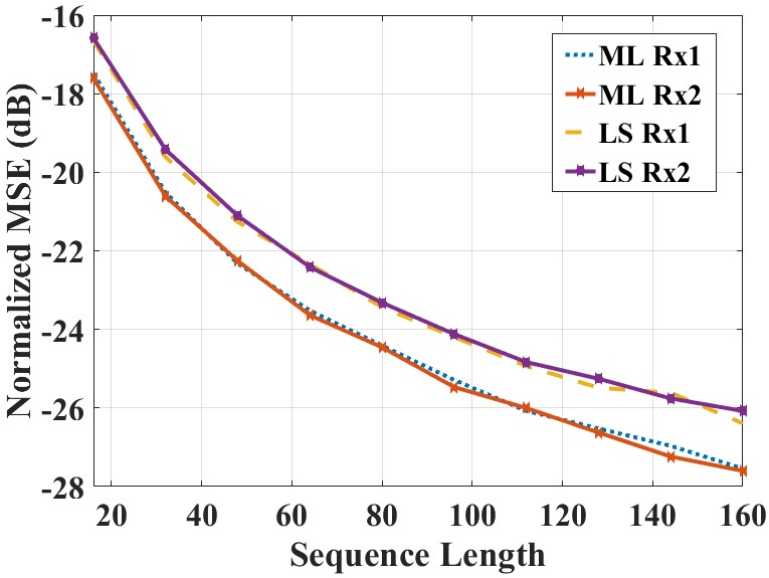

Figure 5.3: Comparison of ML and LS estimators to CRB in terms of MSE in dB vs. the training sequence length K with $L = 3$.

Chapter 6

D-MIMO Receiver Design

The stochastic nature of diffusion and the severe interference makes D-MIMO equalization important for low error detection. All the proposed equalization and detection techniques in this thesis are simple enough to be able to implemented on bio-nano-machines. We consider one-shot detection schemes to reduce the receiver complexity. All the proposed detectors need the full knowledge of CSI or the estimated CIR as discussed in the previous section. Generally, the expected number of molecules at $k-th$ time interval and $j-th$ receive antenna $\bar{y}_j[k]$ consists of two components:

$$\bar{y}_j[k] = x_j[k]\bar{c}_{jj}[0] + \bar{I}_j[k] \tag{6.1}$$

where the first component $x_j[k]\bar{c}_{jj}[0]$ is the information component and $\bar{I}_j[k]$ is the sum of all interference and noise molecules. In D-MIMO systems due to the severe ISIs and ILIs, interference component $\bar{I}_j[k]$ is comparable and even greater than the information component. Considering Eqn. (6.1) we can write

$$\bar{I}_j[k] = \bar{y}_j[k] - x_j[k]\bar{c}_{jj}[0] \tag{6.2}$$

Our goal is to propose receivers which mitigate the interference effect and has a low error probability. In this section we propose three different simple receiver architectures as follow:

6.1 Maximum Likelihood Detection

ML detector is the optimal detection scheme when CSI is available. We perform symbol-by-symbol data detection and it is given by:

$$\hat{x}_j^{\mathrm{ML}}[k] = \underset{x_j[k]\in\{0,1\}}{\operatorname{argmax}} \; f_{y_j[k]}\left(y_j|\bar{\boldsymbol{C}}_j, \boldsymbol{X}[k]\right) \tag{6.3}$$

$$= \underset{x_j[k]\in\{0,1\}}{\operatorname{argmax}} \frac{(\bar{c}_{jj}[0]x_j[k] + \bar{I}_j[k])^{y_j[k]} \exp(-\bar{c}_{jj}[0]x_j[k] - \bar{I}_j[k])}{y_j[k]!}$$

where $f_{y_j[k]}(y_j|\bar{\boldsymbol{C}}_j, \boldsymbol{X}[k])$ is the Poisson distribution function and $\bar{I}_j[k]$ is the sum of the expected number of interference and noise molecules at receiver j and time interval k. The ML detector can be written in the form of a threshold-based detector [49, 48]:

$$\hat{x}_j^{ML}[k] = \begin{cases} 1, & \text{if } y_j[k] \geq \xi_j[k] \\ 0, & Otherwise \end{cases} \tag{6.4}$$

where

$$\xi_j[k] = \frac{\bar{c}_{jj}[0]}{\ln(1 + \frac{\bar{c}_{jj}[0]}{\bar{I}_j[k]})}. \tag{6.5}$$

We note that $\bar{I}_j[k]$ is time variant and it depends on the previous symbols due to ISIs and ILIs. In SISO systems, one can increase the bit interval time to make the interferences negligible. In this case, threshold ξ_j is fixed [49], and the receiver is simple. However, in D-MIMO systems, even if we increase bit interval time to reduce the ISI, performance of the system is affected by the ILI of the current time interval from non-corresponding transmitters. $\bar{I}_j[k]$ is time variant, so we need to develop adaptive equalizers to cancel the effect of the time variant interferences and still keep the receiver architecture simple enough to be implemented on nano-bio-machines.

6.1.1 Blind Equalizer (BE)

Here, we propose a simple blind equalizer (BE) that leads to a comparator with a fixed threshold at each receiver branch during each block of data. $\bar{I}_j[k]$ is the expected interference but it varies over time as mentioned before. BE make an average of $\bar{I}_j[k]$ over the time so it becomes independent from the transmitted bits and it only depends on the CSI. According to 6.2 we can write

$$\begin{aligned} \bar{I}_j^{\mathrm{BE}} &= \mathbb{E}\left[\bar{I}_j[k]\right] = \mathbb{E}\Big[\bar{y}_j[k] - x_j[k]\bar{c}_{jj}[0]\Big] \\ &= \mathbb{E}\Big[\boldsymbol{X}[k]\,\bar{\boldsymbol{C}}_j\Big] - \mathbb{E}\Big[x_j[k]\bar{c}_{jj}[0]\Big] \\ &= \mathbb{E}\Big[\boldsymbol{X}[k]\Big]\,\bar{\boldsymbol{C}}_j - \mathbb{E}\Big[x_j[k]\Big]\bar{c}_{jj}[0] \\ &= \boldsymbol{p}^T\,\bar{\boldsymbol{C}}_j - p \times \bar{c}_{jj}[0] \end{aligned} \tag{6.6}$$

where $p = Pr\{x_i[k] = 1\}$ and $\boldsymbol{p}$ is a $(LM+1)\times 1$ vector where all of its entries are p. Generally, we set the $p = 0.5$, means that transmitted bits x_i can be 0 or 1 with equal probabilities. Even if blind equalizer is very simple but the error probability is high.

6.1.2 Decision Feedback Equalizer (DFE)

Decision feedback equalizer is a nonlinear equalizer that exploits the a priori information of the previously decoded bits and it can greatly improves the detection of the current time interval. In principle, we use the history to approximate the interference and we remove it from the current values. Therefore, we are mitigating the impact of channel memory on detection. Fig. 6.1 shows the block diagram of a ML-DFE receiver with M receive antennas. According to Eqn. 6.2, $\bar{I}_j[k]$ is time variant and it depends on previous symbols. Hence, the threshold $\xi_j[k]$ should adapt itself at each bit interval time such that the overall bit error rate decreases. We define feedback vector at time k as

$$\tilde{\boldsymbol{X}}[k] = [\hat{\boldsymbol{x}}^T[k-1], ..., \hat{\boldsymbol{x}}^T[k-L+1], 1]^T \tag{6.7}$$

where $\hat{\boldsymbol{x}}[k-\ell]$ is the decoded sequence at time $k-\ell$. Therefore, we have

$$\hat{\bar{I}}_j^{\mathrm{DFE}}[k] = [\bar{\boldsymbol{x}}_j^T, \tilde{\boldsymbol{X}}^T[k]]\,\bar{\boldsymbol{C}}_j \tag{6.8}$$

where $\bar{\boldsymbol{x}}_j = [p, p, ..., 0, ..., p]$ is a $M \times 1$ vector that all of its entries are p except the $j-th$ entry which is 0 to prevent including $\bar{c}_{jj}[0]$ as interference while its is the desired information. Blind equalization is used for the ILI of the current time interval, because we do not have any information or feedback regarding what is sent at the current time. DFE is more sophisticated equalizer compare to BE, but it is still simple enough to be implemented on nano-machines and it improves the performance compare to the BE.

6.2 Least-Squares Detection based on DFE (LSD-DFE)

Least-Squares Detector (LSD) finds the vector $\hat{\boldsymbol{x}}[k] = [\hat{x}_1[k], ..., \hat{x}_M[k]]^T$, $\hat{x}_i[k] \in \{0, 1\}$, that minimizes the sum of square errors based on the observed number of molecules and their expectation values.

$$\hat{\boldsymbol{x}}^{LS}[k] = \underset{\boldsymbol{x}[k]}{\operatorname{argmin}} \ \|\boldsymbol{\epsilon}\|^2. \tag{6.9}$$

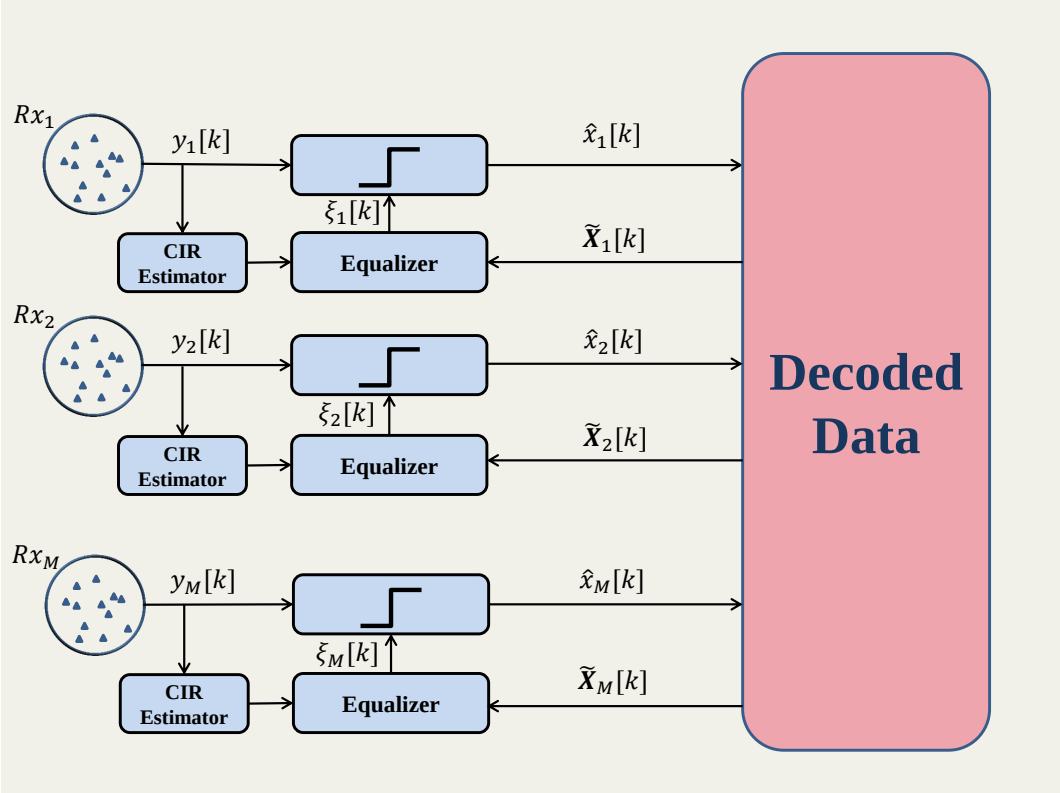

Figure 6.1: ML-DFE receiver architecture of a D-MIMO system with M receive antennas. Equalizers generate the threshold values at each bit interval time using estimated CIR and the feedback of previously decoded bits.

where $\boldsymbol{\epsilon} = \boldsymbol{y}[k] - \left[\boldsymbol{x}^T[k], \tilde{\boldsymbol{X}}^T[k]\right]\bar{\boldsymbol{C}}$. Here, $\tilde{\boldsymbol{X}}[k]$ is the feedback vector (Eqn. 6.7) and it is known. The LSD detector finds the vector $\boldsymbol{x}[k]$ which minimizes the error probability. LSD-DFE has the best performance compares to the other methods, because DFE mitigates the ISIs and ILIs from previous transmissions, and LSD mitigates the ILI for the current transmission from non-corresponding transmit antennas. The complexity of the receiver increases with the number of receive antennas M. However, in real cases, M is not a big number and the receiver configuration remains simple.

6.3 Performance Analysis with full knowledge of CSI

In this section we provide the numerical results for different equalization and detection techniques proposed in previous sections. In this section we have assumed CSI is available. The impact of system parameters on the performance of the system is analyzed. Fig. 5.1 shows the system configuration which is used in this section. All results are obtained via Monte-Carlo simulation with high number of trials.

Fig. 6.2 compares the performance of the D-MIMO system with $T_{int} = 0.2\,ms$, $N = 10^5$ and $h = 400\,nm$ in terms of BER vs. transmitter-receiver distance d. It can be seen that BER increases when distance increases, because fewer molecules reach the receive antennas. The more molecules reach the receiver, the lower BER is obtained. Among the proposed detectors, ML-BE has the highest BER and the performance is not acceptable for great distances but in small distances it is favorable as it has low complexity. LSD-DFE has the lowest BER in expense of more complex architecture. We highlight that all three detectors are so sensitive to the number of received molecules. It means that when enough molecules do not reach the receivers, system performance degrades drastically.

Fig. 6.3 shows the performance of the D-MIMO system with $T_{int} = 0.2\,ms$, $d = 400\,nm$ and $N = 10^5$, in terms of BER vs. antennas inter-distance h. ILI becomes negligible when h increases, so the BER decreases.

Fig. 6.4 compares the performance of the D-MIMO system with $T_{int} = 0.2\,ms$, $d = 400\,nm$ and $h = 400\,nm$ in terms of BER vs. number of released molecules N. When more molecules are transmitted, more molecules reach the receiver and consequently BER decreases. It can be seen that ML-DFE and LSD-DFE are so sensitive to the number of released molecules and the BER

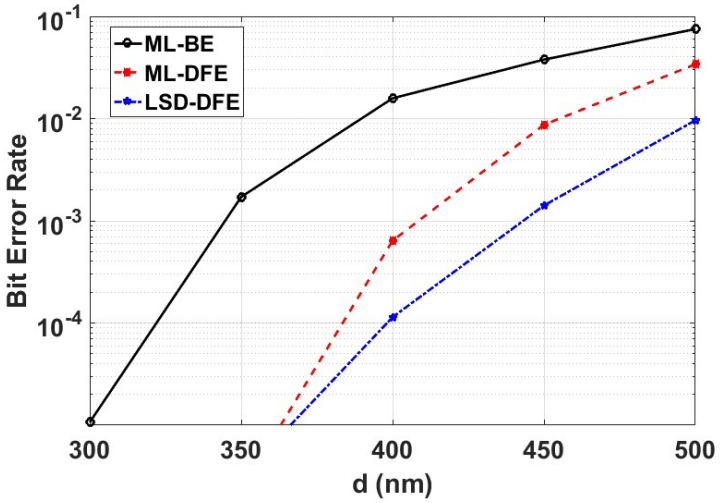

Figure 6.2: BER vs. d transmitter-receiver distance for 2×2 D-MIMO system where $T_{int} = 0.2\,ms$, $N = 10^5$ and $h = 400\,nm$.

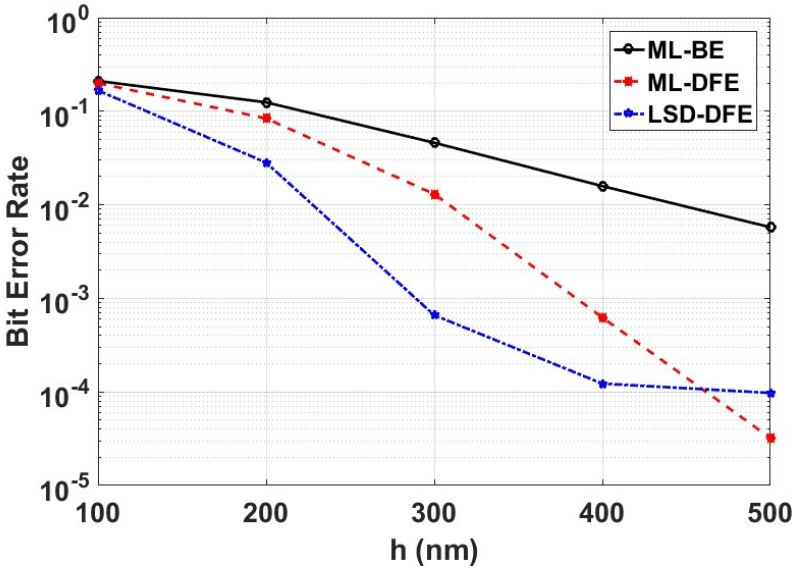

Figure 6.3: BER vs. h antennas inter-distance for 2×2 D-MIMO system where $T_{int} = 0.2\,ms$, $N = 10^5$ and $d = 400\,nm$

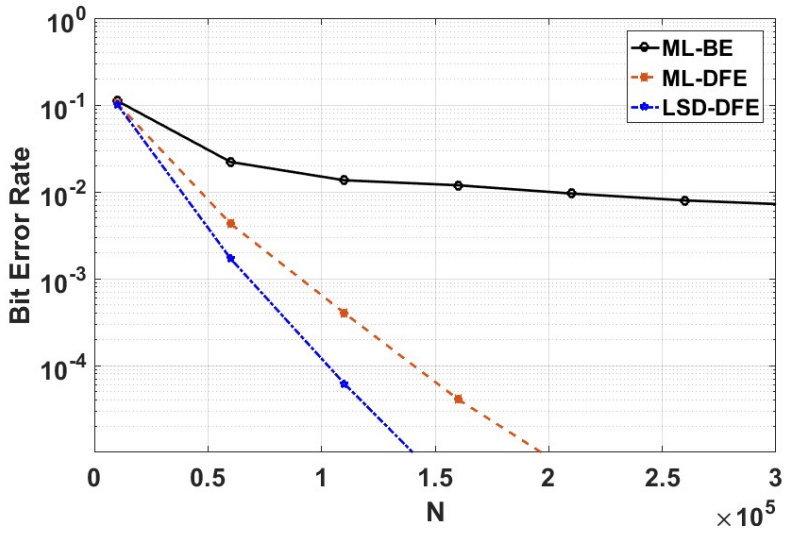

Figure 6.4: BER vs. N number of released molecules for 2×2 D-MIMO system where $T_{int} = 0.2\,ms$, $h = 400\,nm$ and $d = 400\,nm$

decreases rapidly when higher number of molecules reach the receivers.

Fig. 6.5 compares the performance of the D-MIMO system with $d = 400\,nm$, $h = 400\,nm$ and $N = 10^5$ in terms of BER vs. bit interval time T_{int}. Increasing the bit interval time does not affect the expected number of received molecules $\bar{\boldsymbol{c}}_{jj}[0]$, but it decreases the interference and consequently the BER decreases. Equalizers mitigate the ISI impact for bit interval time greater than $0.2\,ms$ and the BER becomes flat. The existing error probability is due to the noise and the stochastic nature of diffusion. Again, LSD-DFE has the best performance and ML-BE has the worst.

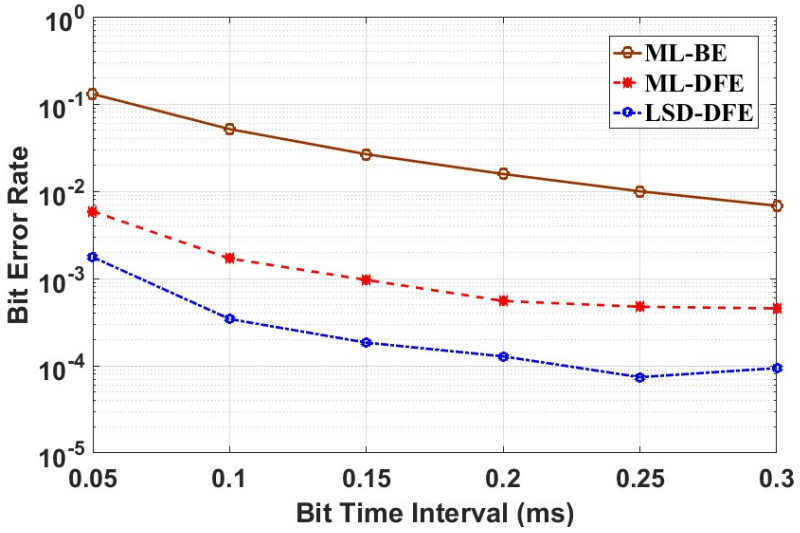

Figure 6.5: BER vs. T_s bit interval time for 2×2 D-MIMO system where $N = 10^5$, $h = 400\,nm$ and $d = 400\,nm$

Chapter 7

MIMO Time Interleaving Modulation Technique

MC systems suffer from severe interferences. In D-SISO MC system, one can increase the bit interval time to mitigate the interference, but it leads to a low bit rate system. Therefore, MIMO technique is proposed to address the slow nature of diffusion. However, D-MIMO MC systems suffer severely from the ILI in addition to the ISI. The overall performance of the system, as bit error rate, is related to the sum of interferences and noise in the receiver. To reduce the ILI, one can put transmit antennas far from each other. But, it is not realistic to do so, because the transmitter size would be large and comparable with the transmitter-receiver distance. In conventional MIMO communication systems, the electromagnetic wavelength in microwave regime is very small compare to the transmitter-receiver distance. Therefore, even if we consider antennas inter-distance in the range of several wavelength, but the overall transmitter size is much smaller than transmitter-receiver distance. In D-MIMO MC systems, to mitigate the interlink interference and attain an acceptable bit error rate, antennas inter-distance should be in the range of transmitter-receiver distance which is considered the weakness of using MIMO technique.

We propose to address the problem by using time interleaving (TIL) modulation technique to reduce the ILI. Normally, all transmit antennas release molecules simultaneously at the beginning of each bit interval time, so the ILI is severe at the receive antennas. However, one can configure the system such that each antenna transmits at different time sequences during the bit interval time and each receive antenna is synchronized with its corresponding transmit

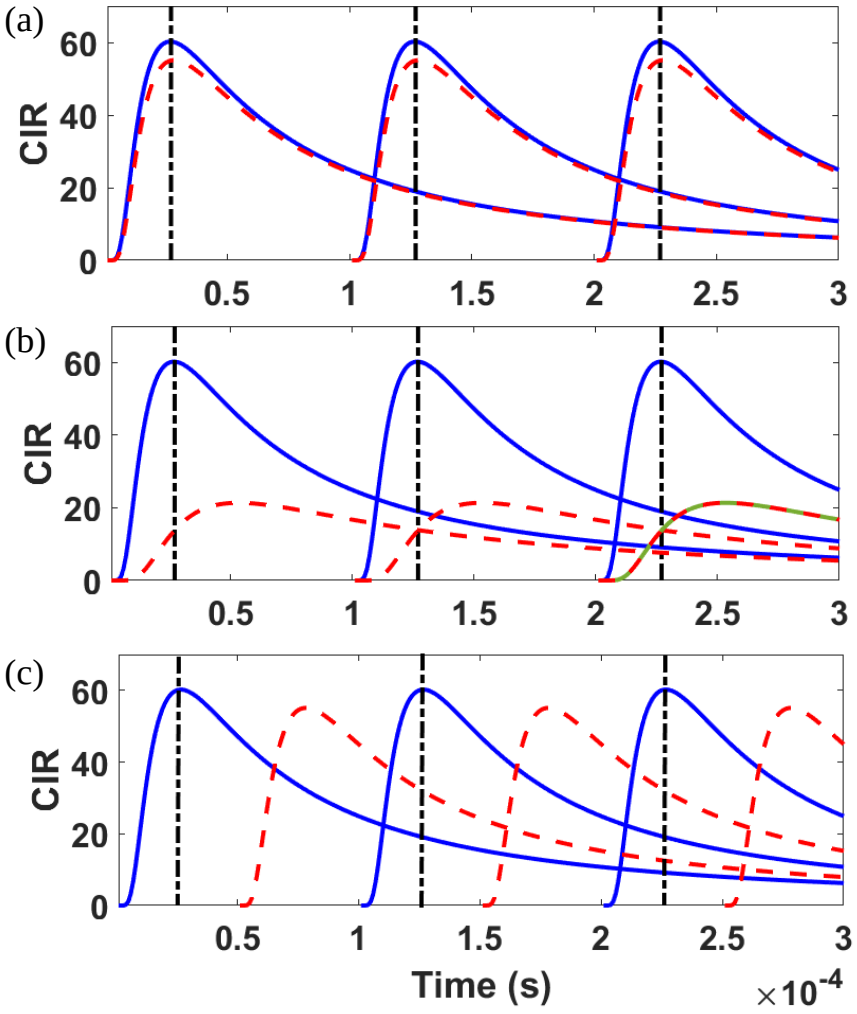

Figure 7.1: Channel impulse response of a 2×2 D-MIMO system at Rx_1 when $d = 400\,nm$, $T_{int} = 0.1\,ms$ and (a) $h = 100\,nm$, (b) $h = 400\,nm$. For figure (c) $h = 100\,nm$ and Tx_2 transmit with an offset time equal to $T_{off} = T_{int}/2$ respect to the Tx_1. Solid lines refer to the CIR of the corresponding transmitter Tx_1 and dashed line refer to the CIR of Tx_2 which is considered as ILI.

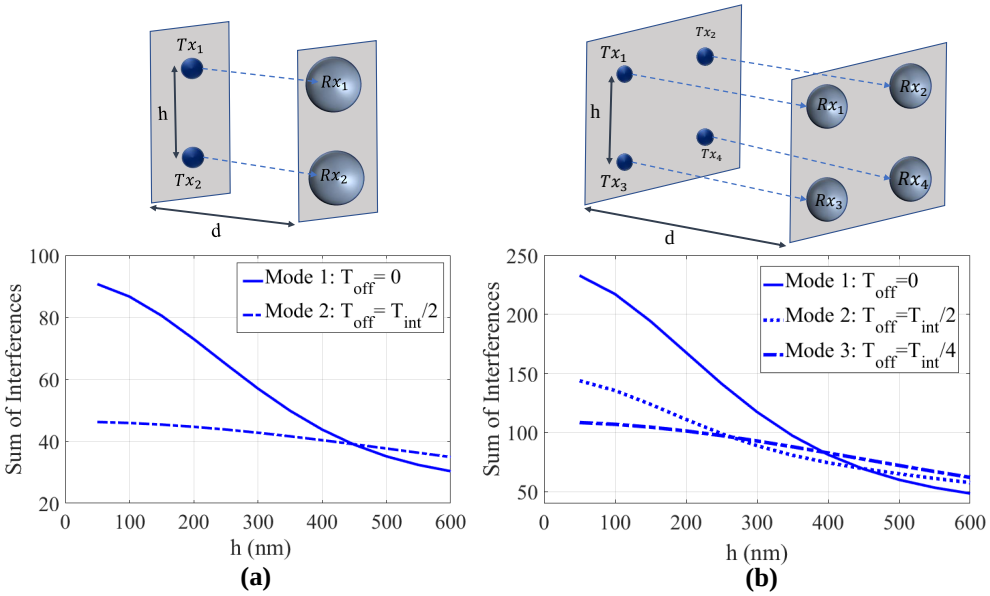

Figure 7.2: (a) Maximum expected interference for a 2×2 D-MIMO system, $\sum_{i=1,i\neq j}^{LM+1} \bar{\boldsymbol{C}}_j(i)$, vs. h when $d = 400\,nm$ and $N = 10^5$. Mode 1 refers to the case when both antennas transmit simultaneously at the beginning of each bit interval time and mode 2 refers to the case when Tx_2 transmit with an offset time equal to $T_{off} = T_{int}/2$ respect to the Tx_1. (b) maximum expected interference for a 4×4 D-MIMO system, $\sum_{i=1,i\neq j}^{LM+1} \bar{\boldsymbol{C}}_j(i)$, vs. h when $d = 400\,nm$ and $N = 10^5$. Mode 1 refers to the case when all 4 antennas are transmitting simultaneously, mode 2 refers to the case when Tx_2 and Tx_2 transmit simultaneously with an offset time equal to $T_{off} = T_{int}/2$ respect to the Tx_2 and Tx_3, and mode 3 refers to the case when each antenna transmits with an offset time equal to $T_{off} = T_{int}/4$ respect to others.

antenna. In this proposed scheme, bit interval time and bit rate are the same as before, but the ILI and bit error rate reduce effectively and it allows us to keep the transmitter size small. CIR estimation for the proposed modulation technique is same as before, because in section (III), we did not put any constraint on the CIR to be estimated. TIL modulation technique just puts an offset time in releasing molecules at transmit antennas, so all the previous relations are valid here.

Fig. 7.1 shows the CIR for a 2×2 D-MIMO system with $d = 400\,nm$, $T_{int} = 0.1\,ms$ and $N = 10^5$. Fig. 7.1 (a) refers to the case when antennas inter-distance is $h = 100\,nm$. It can be seen that ILI is so severe and it will degrades system performance. As described before, we can reduce the ILI by putting the transmit antennas far from each other. Fig. 7.1 (b) refers to the case when $h = 400\,nm$. In this case, ILI is reduced but the distance between transmit antennas is equal to the transmitter-receiver distance and this is not favorable. Fig. 7.1 (c) refers to the case when $h = 100\,nm$ and Tx_2 transmit with an offset time equal to $T_{off} = T_{int}/2$ respect to the Tx_1. It can be seen that the ILI is reduced considerably.

Fig. 7.2 shows a 2×2 and a 4×4 D-MIMO system with $d = 400\,nm$ and $T_{int} = 0.2\,ms$. Fig. 7.2 (a) shows the maximum expected interference vs. h for 2×2 D-MIMO system. Mode 1 refers to the case when both antennas are releasing molecules simultaneously at the beginning of each bit interval time and mode 2 refers to the case when Tx_2 is transmitting with an offset time equal to $T_{off} = T_{int}/2$ respect to the Tx_1. We note that we have assumed that receive antennas are synchronized with their corresponding transmit antennas, means they count the number of molecules when CIR of the corresponding antenna is expected to be maximum. Fig. 7.2 (b) shows the maximum expected interference vs. h for a 4×4 D-MIMO system. Mode 1 refers to the case when all 4 antennas are transmitting simultaneously, mode 2 refers to the case when Tx_1 and Tx_4 transmit simultaneously at the beginning of bit interval time and Tx_2 and Tx_3 transmit simultaneously with an offset time equal to $T_{off} = T_{int}/2$, and mode 3 refers to the case when Tx_1 transmit at the beginning of the bit interval time and each antenna transmits with an offset time equal to $T_{off} = T_{int}/4$ with each other. It can be seen that the proposed TIL technique reduces the interference greatly for both 2×2 and 4×4 D-MIMO systems. We remark that TIL is effective when antennas are close to each other. There is an inherent delay in ILI component which becomes notable when transmit antennas are far. Fig. 7.1 (b) shows that the ILI component has a delay compare to the desired component, so the ILI is reduced because

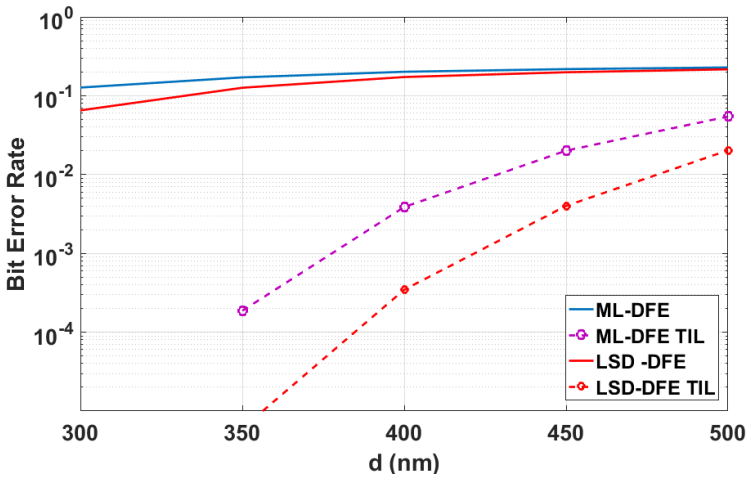

Figure 7.3: Comparing LSD-DFE and ML-DFE detector performance in terms of BER vs. transmitter-receiver distance d with/without using TIL modulation technique at transmitter. A 2×2 D-MIMO system with $h = 100\,nm$, $T_{int} = 0.2\,ms$ and $N = 10^5$ is considered here.

of the inherent delay of molecules to reach the non-corresponding receiver. In this case, TIL puts an additional offset time where adversely affect the inherent delay and increases the ILI. Fig. 7.2 shows that Mode 1 overcomes the other modes when h is greater than $400\,nm$. Therefore, it is suggested to use the TIL modulation technique when antennas inter-distance are small.

7.1 Performance Analysis

MIMO TIL modulation technique reduces the ILI and it let us reduce the antennas inter-distances and keep the transmitter size rationally small. It can be seen in Fig. 7.3 that for small antennas inter-distance like $h = 100\,nm$, performance of the system without using TIL modulation technique is unbearable, while TIL cancel the ILI and it improves the BER. Fig. 7.4 shows the numerical results for a 2×2 D-MIMO system with $d = 400nm$, $T_{int} = 0.2\,ms$ and $N = 10^5$. As we can see, the BER for ML-DFE and LSD-DFE is much lower when TIL is used at the transmitter. In this case, as h increases, the BER reduces very smoothly, because TIL reduce the ILI but it does not reduce the ISI. Therefore, the BER is due to the existence of ISI and also the stochastic nature of diffusion. When h increases to $400nm$, TIL won't improve the BER,

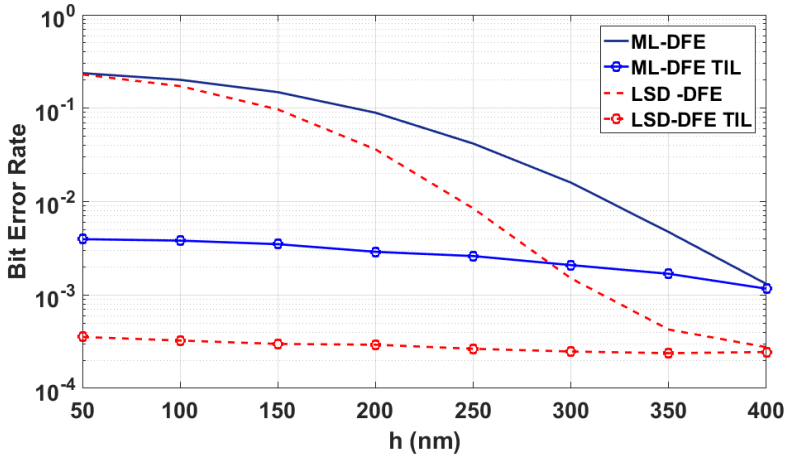

Figure 7.4: Comparing LSD-DFE and ML-DFE detector performance in terms of BER vs. antennas inter-distance h with/without using TIL modulation technique at transmitter. A 2×2 D-MIMO system with $d = 400\,nm$, $T_{int} = 0.2\,ms$ and $N = 10^5$ is considered here.

because in this case ILI impact is so negligible. When $h = 50\,nm$, the BER for normal transmitter is unacceptably high, but TIL let us to put antennas close together and keep the transmitter size small.

Chapter 8

Block-Type Communication for Molecular Systems

In this chapter we develop a block-type communication where the transmitter sends a block of data at each block time interval inspired by conventional communication systems. This chapter incorporate all previous chapters simultaneously.

CIR is estimated at the beginning of each block and then it is used during the rest of the block for equalization. Transmit antennas send the designed training sequences through the diffusion channel and the receive antennas counts the number of molecules. CIR estimator block, estimates the channel by knowing the training sequence and the number of molecules each antenna has counted. Then the equalizer block use the estimated CIR for equalization in the rest of the block. The accuracy of the estimated CIR is related to the training sequence length. It is expected that BER is higher compare to the ideal case when CSI is available at the receiver. The performance of the system would reach to the ideal case where CSI is available if accuracy of the estimated CIR is good enough.

In this section we analyze the performance of a 2×2 and a 4×4 D-MIMO system. Block-type communication is assumed where block length is $B = 10000$ bits. All results shown in this section are obtained by analyzing the 1000 block of data which transmitted over the system. Optimized training sequence with length $K_{tot} = M \times K$ is transmitted at the beginning of each block. In this section the training sequence length at each transmit antenna $K = 64$ is considered. In detail, training sequence with length $K_1 = 16$ is designed and then it is concatenated 4 times to build the training sequence

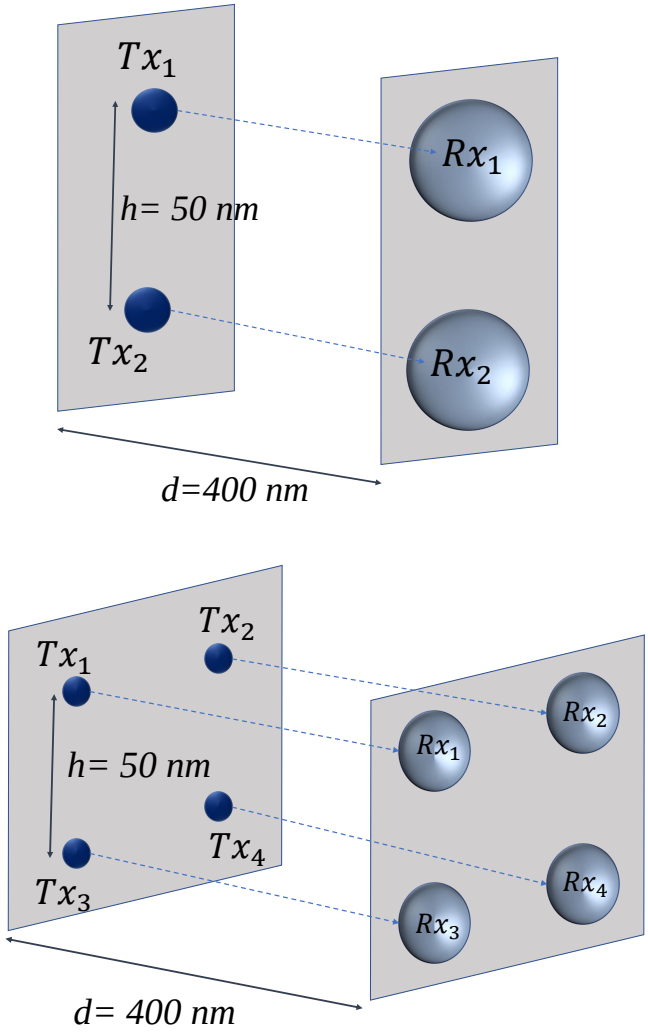

Figure 8.1: Geometrical configuration of a 2×2 and 4×4 D-MIMO system with system parameters summarized in Table 8.1.

Table 8.1: Diffusive MIMO system parameters for the configurations of Fig. 8.1

Parameter	Symbol	Value
Transmitter-receiver distance	d	400 nm
Antennas inter-distance	h	50 nm
Diffusion coefficient	D	$10^{-9}\ \frac{m^2}{s}$
Receiver radius	r_{obs}	50 nm
# of released molecules	N	10^5 molecules
Block length	B	10000 bits
Channel coherence time	T_c	1 s
Training sequence length	$K_{tot} = K \times M$	$64 \times M$

with length $K = 64$. All the system parameters are summarized in Table 8.1. Channel coherence time is assumed $T_c = 1$ s, where it is rational time for most MC environments. In all simulations below, the time which is used to transmit the block of data is lower than channel coherence time

$$\frac{B \times T_{int}}{M} \leq T_c \tag{8.1}$$

where B is the block length and T_{int} is the bit time interval.

Fig. 8.1 shows the geometrical configuration of a 2×2 and 4×4 D-MIMO system with system parameters summarized in Table 8.1. In this section the effect of bit interval time T_{int} on throughput is studied. Both systems use TIL modulation technique to decrease the ILI and to put transmit antennas close together. The 2×2 D-MIMO system uses Mode 1 where $T_{off} = T_{int}/2$, it means that Tx_1 transmit at the beginning of the bit interval time and Tx_2 transmit with an offset time T_{off} after the Tx_1. The 4×4 D-MIMO system uses TIL modulation technique Mode 2 where $T_{off} = T_{int}/4$ and it means that each transmit antenna release molecule with an offset time T_{off} after the previous antenna.

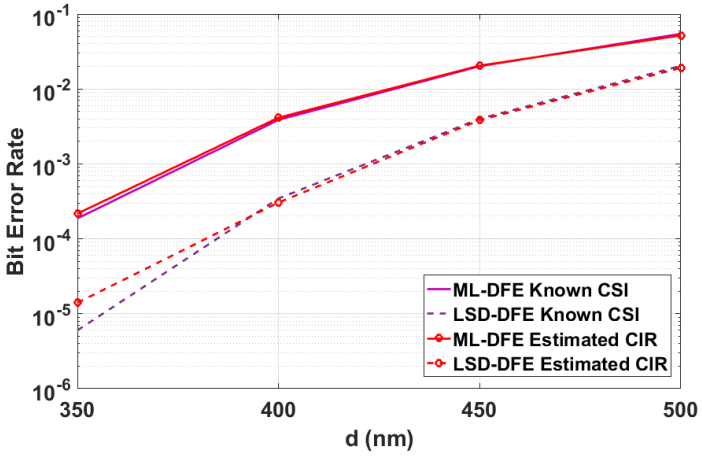

Figure 8.2: Performance comparison of a 2×2 D-MIMO system with $d = 400\,nm$, $h = 100\,nm$, $T_{int} = 0.2\,ms$ and $N = 10^5$ In case of full channel knowledge and estimated CIR when training sequence length is $K = 64$ for each transmit antenna and a total of $K_{tot} = 2 \times 64 = 128$

8.1 CIR Estimation Effect on System Performance

In this section we investigate the system performance considering the estimated CIR. Fig. 8.2 shows the numerical simulation for a 2×2 D-MIMO system with $T_{int} = 0.2\,ms$, $h = 100\,nm$ and $N = 10^5$. The performance of the system is evaluated in terms of BER vs. the transmitter-receiver distance d. We have assumed $K = 64$, so the total number of $K_{tot} = 64 \times 2 = 128$ bit are used for CIR estimation at each block. The accuracy of the estimated CIR is good enough that BER reaches to the BER of the ideal case when CSI is available at the receiver. The price that is paid to reach the ideal case is wasting 1.28% of the block information for CIR estimation.

Fig. 8.3 shows the performance of the system in terms of BER vs. training sequence length K. It can be seen that as K increases, the BER decreases. The good news is that the system is not highly sensitive to the K. In detail, after $K = 32$, the BER decreases very smoothly. According to the system requirements,we do not need to invest a long training sequence to reach to an acceptable BER. Fig. 8.4 shows the throughput of the system vs. the training sequence length. The throughput decreases as K increase, because

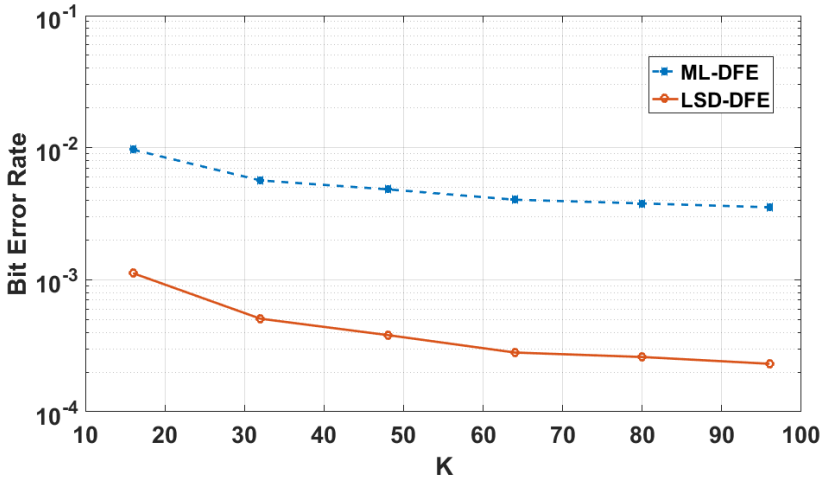

Figure 8.3: Performance of a 2×2 D-MIMO system in block-type communication with block length 1000. (a) BER vs. training sequence length K. (b) Throughput vs. Training sequence length K

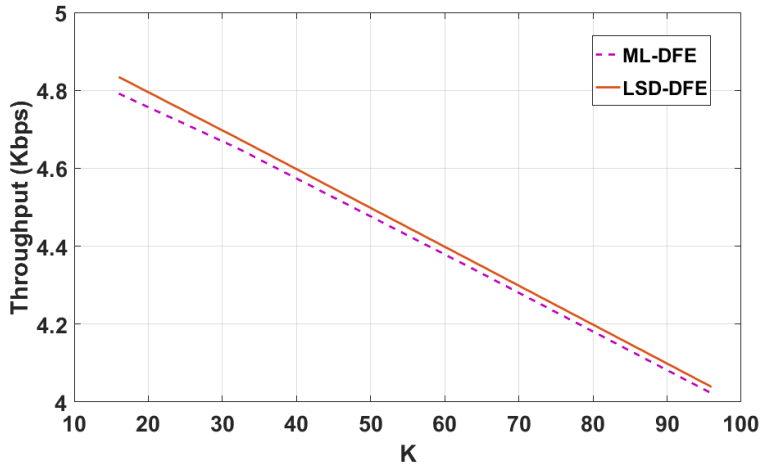

Figure 8.4: Performance of a 2×2 D-MIMO system in terms of BER vs. training sequence length K in block-type communication with block length 1000. Throughput vs. Training sequence length K

as K increase, the BER improvement is negligible, but number of information bits decrease, means that we are wasting more molecules for CIR estimation.

8.2 Throughput Analysis

In this section we analyze the throughput of the system in respect to the bit interval time for a 2×2 and 4×4 D-MIMO system as shown in Fig. 8.1. The throughput is defined as the number of information bits where receiver decoded correctly in unit of time. The throughput is lower than the data rate since training sequence are sent for CIR estimation.

Fig. 8.5 shows the throughput of a 2×2 D-MIMO system vs. bit interval time. Bit rate is defined as $\frac{1}{T_{int}}$. We can see that the system throughput for 2 different detectors are lower than the bit rate as expected. As we have seen before, LSD-DFE detector outperforms the ML-DFE detector at the expense of higher complexity. When bit interval time is low , e.g. $T_{int} = 0.08$ ms , the interference is so severe and as shown in Fig. 8.6, the BER is so high. Therefore, as expected we lose more than 1 Kbps throughout compare to bit rate. When bit interval time is high, e.g. $T_{int} = 0.2$ ms, the ISI is low and as shown in Fig. 8.6, the BER is low. Therefore, the throughput of the system gets close to the bit rate. Throughput never reaches the bit rate, because 128 bits of 10000 bits are used for channel estimation. However, the system does not need so many bits for channel estimation and the efficiency of the system is high enough and throughput gets really close to the bit rate.

Fig. 8.7 shows the throughput of a 4×4 D-MIMO system vs. bit interval time. It can be seen that for a 4×4 D-MIMO system data rate is 2 times of the 2×2 system. It can be seen that LSD-DFE outperforms the ML-DFE detector and its throughput is higher at the expense of a more complex architecture. We can see that throughput never reaches the bit rate, because $K_{tot} = 4 \times 64 = 256$ bits out of 10000 bits are used for channel estimation. When bit interval time is low $T_{int} = 0.1$ ms, the interference is so severe and as it is shown in Fig. 8.8, the BER is so high and unacceptable and we lose at least 5 Kbps compare to the bit rate. For big values of bit interval time, e.g. $T_{int} = 0.3$ ms, the interference decreases and BER is low. Therefore, the throughput gets close to the bit rate but it never reaches to the bit rate because we have used 256 bits for channel estimation.

Fig. 8.9 compares the throughput of a 2×2 and 4×4 D-MIMO system when LSD-DFE detector is used at the receiver. System parameters for both architecture are the same and it is summarized in Table 8.1 and configurations

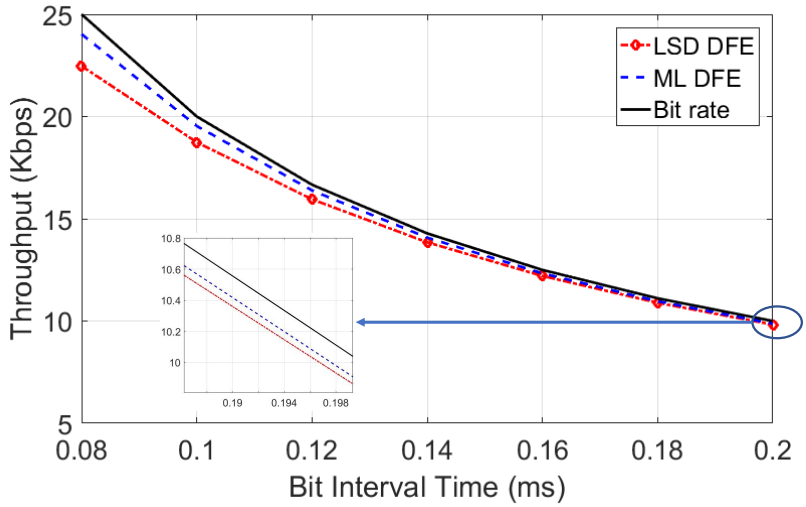

Figure 8.5: Throughput vs. bit interval time T_{int} of a 2×2 D-MIMO system with system parameter summarized in Table 8.1 and the configuration is shown in Fig. 8.1.

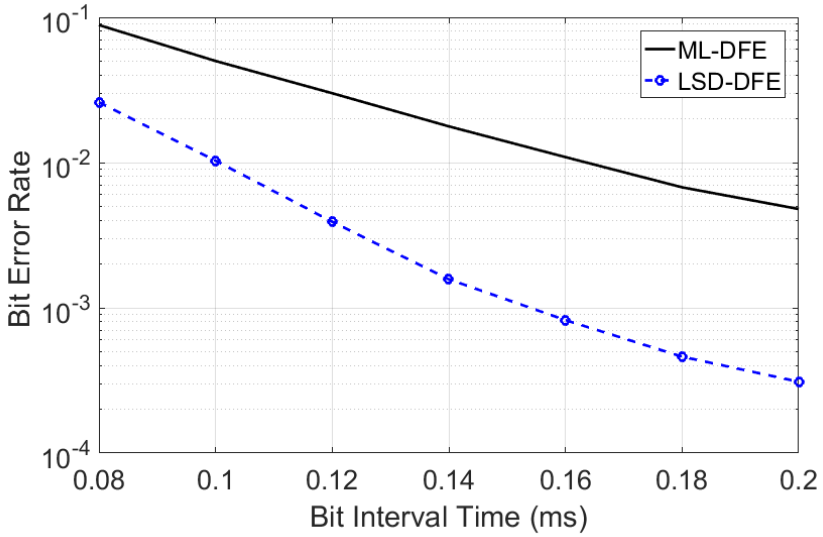

Figure 8.6: Bit error rate vs. bit interval time T_{int} of a 2×2 D-MIMO system with system parameter summarized in Table 8.1 and the configuration is shown in Fig. 8.1.

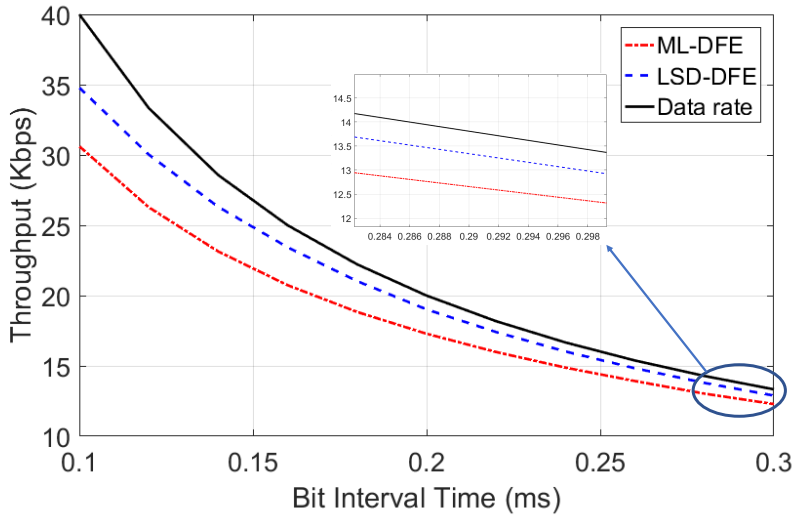

Figure 8.7: Throughput vs. bit interval time T_{int} of a 2×2 D-MIMO system with system parameter summarized in Table 8.1 and the configuration is shown in Fig. 8.1.

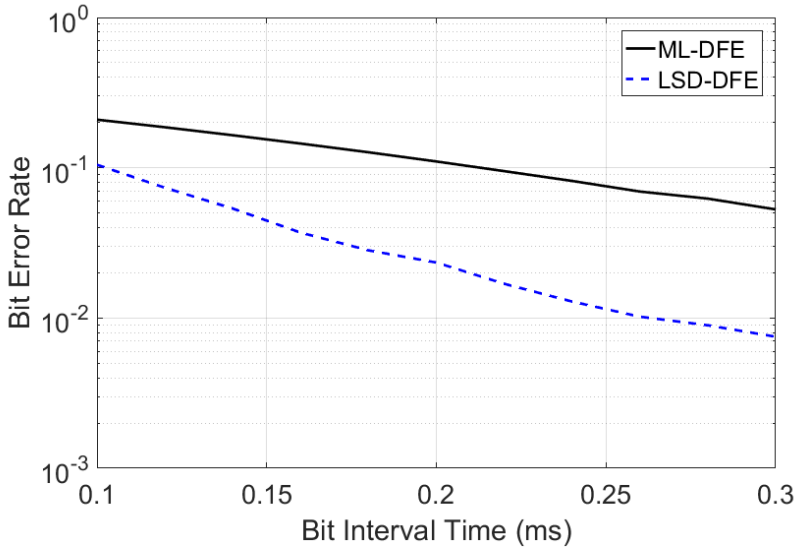

Figure 8.8: Bit error rate vs. bit interval time T_{int} of a 4×4 D-MIMO system with system parameter summarized in Table 8.1 and the configuration is shown in Fig. 8.1.

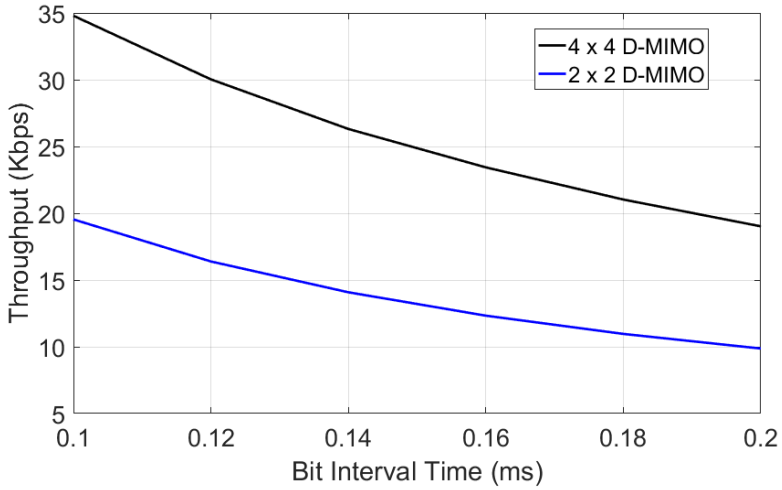

Figure 8.9: Comparison of throughput vs. bit interval time T_{int} of a D-MIMO system with LSD-DFE detector. System parameter summarized in Table 8.1 and the configuration is shown in Fig. 8.1.

are shown in Fig. 8.1. We can see that when bit interval time is low $T_{int} = 0.1$ ms, the throughput of the 4×4 system is 1.75 times of the 2×2 system while for larger bit interval time as $T_{int} = 0.2$ ms, the throughput of the 4×4 is 1.9 times higher than the throughput of the 2×2 system. It can be concluded that 4×4 D-MIMO system is more prone to the interference than the 2×2 system.

Chapter 9

Conclusions and Future Works

9.1 Conclusions

In this thesis a pragmatic approach to design a D-MIMO MC system is proposed. Slow nature of diffusion and the thirst for higher data rate makes us to incorporate MIMO technique. Diffusion channel is so complex and we can not provide a close-form solution to obtain the CIR. This thesis introduce the channel estimation for D-MIMO molecular communication channels. Maximum Likelihood and Least Squares channel estimators are presented. Cramér-Rao bound is derived and we showed that the performance of the ML estimator reach to the CR bound with an optimized training sequence at the expense of high receiver complexity. The least squares channel estimator is preferred due to its low complexity with the expense of around 1 db performance degradation.

This thesis presents different detection and equalization techniques. Maximum likelihood detection is proposed and it leads to s simple threshold detector. Generally the threshold is not constant and it varies at every bit interval time. Blind equalizer is proposed where it makes the average of the threshold over time and gives a fixed threshold to be used for all time slots. Blind equalizer is very simple to implement but it has a high error probability when the interference is severe. Decision feedback equalizer is introduced to mitigate the effect of inter-symbol interference. DFE improves the performance of the receiver, but when the inter-link interference is too high, we experience a performance degradation. Finally, least square detector based on DFE is proposed to mitigate the ISI and ILI simultaneously. LSD-DFE has the best performance among the others and it has a low complexity. The complexity

increases with the number of transmit and received antennas.

MIMO time interleaving modulation technique has been proposed to reduce the ILI and it gives us the opportunity to decreases the antennas inter-distance at transmitter. Actually, we make an offset time between the release of molecules in MIMO setting instead of the normal case where all transmit antennas release molecules simultaneously.

Finally, we investigated the block-type communication where transmitter sends a block of data during each block interval time. At the beginning of each block, a designed training sequence is transmitted and the receiver counts the molecules and estimate the channel. The estimated CIR then is used for the rest of the block for equalization and detection. Results show that even with small length of training sequence we can reach to a good performance.

9.2 Future Works

This thesis was so inspiring for me and there were many ideas that I would like to follow and include them in this thesis. However, due to the time and space constraint, I will explain them below for the reference of future works. I divide my ideas into three categories of channel estimation, modulation technique and equalization and detection. In the following, I will discuss each part separately.

9.2.1 Channel Estimation

In thesis we have investigated the channel estimation for diffusive MIMO molecular communications. We have assumed that statistical knowledge of the diffusive channel is not available. Therefore, the proposed ML and LS channel estimators, estimate the CIR for every block assuming there is no information available from the channel. However, there are three ideas where we can investigate further and it is described below.

Adaptive Channel Estimator

We can use the information of the estimated CIR of the previous block. In details, we can assume the channel would not change dramatically in two consecutive block of data. Therefore we can write

$$\bar{C}_j[p] = \bar{C}_j[p-1] + \delta_j[p] \tag{9.1}$$

where $\bar{C}_j[p]$ is the CIR for the j-th receiver during the p-th block of data and $\delta_j[p]$ is the variation of the channel for the current block. The channel variation can be estimated according to the observed number of molecules durin training sequence design transmission. The idea is to propose an adaptive channel estimation where it estimates the variation of the channel instead of estimating the full channel. In this proposed scheme, we can use the RLS algorithm to calculate the channel variations. We have done some simulations and it is observed that the performance of the system would depend on the step size.

Channel Estimation with Statistical knowledge of the Channel

We can use the history and previous estimated CIRs in order to provide a statistical channel knowledge to be used for current block CIR estimation. When there is full statistical channel knowledge available, we can derive the maximum a-posteriori (MAP) estimator for CIR estimation. When full channel statistical knowledge is not available and only first and second order statistic is at hand, we can derive the linear minimum mean square errors (LMMSE) estimator. In both case, we will increase the accuracy of the channel estimation by incorporating some useful information from past.

Feedback Chanel Estimation

In this subsection, we introduce a new method that incorporates the feedback of decoded data at previous block to estimate the channel at the current block interval. The idea is to prohibit transmitting a large overhead. As it is expected, all decoded bits are not correct. However, we have seen that CIR estimation problem is not so much sensitive. For example, when BER is equal 10^{-2}, we can say in average we have 1 bit error in decoding 100 bits. It is observed that we can reach to a good CIR estimation accuracy in this case. This method is so efficient in environments where MC channel is not varying so fast.

9.2.2 Modulation Technique

In this thesis, information is encoded in the number of molecules. However, There are several works in the literature which has encoded the molecules in the time of release. The performance of the diffusive MC system is highly related to the number of received molecules. Pulse position modulation (PPM)

is highly investigated in the literature at optical communication Jargon. The same approach can be adopted for MC systems. It means that we can encode the information both in time and concentration of molecules. PPM modulation technique also can be used at D-MIMO transmitter. PPM modulation does not transmit at all time slots, and this feature makes it suitable for D-MIMO systems to mitigate the interference. Therefore, PPM modulation decreases the interference and increases the throughput of the D-MIMO MC system simultaneously.

9.2.3 Equalization and Detection

This thesis investigates one-shot detection for its simple architecture. There are many published works in the literature regarding sequence detection. However, most of them has high complexity and it is not suitable for MC systems where nanomachines have limited capabilities. D-MIMO sequence detection with simple architecture needs to be more investigated.

Moreover, all the proposed detectors are so much sensitive to the number of received molecules and they need high number of molecules to be transmitted at each bit interval. However, the number of molecules at transmitter storage is limited. Therefore, we have to propose new detectors and modulation techniques where they are more molecularly efficient compared to the current ones and has a good performance.

Bibliography

[1] Tatsuya Suda et al. "Exploratory research on molecular communication between nanomachines". In: *Genetic and Evolutionary Computation Conference (GECCO), Late Breaking Papers*. Vol. 25. 2005, p. 29.

[2] Tadashi Nakano et al. "Molecular communication for nanomachines using intercellular calcium signaling". In: *Nanotechnology, 2005. 5th IEEE Conference on*. IEEE. 2005, pp. 478–481.

[3] Nariman Farsad et al. "A comprehensive survey of recent advancements in molecular communication". In: *IEEE Communications Surveys & Tutorials* 18.3 (2016), pp. 1887–1919.

[4] Ian F Akyildiz, Fernando Brunetti, and Cristina Blázquez. "Nanonetworks: A new communication paradigm". In: *Computer Networks* 52.12 (2008), pp. 2260–2279.

[5] Tadashi Nakano et al. "Molecular communication and networking: Opportunities and challenges". In: *IEEE transactions on nanobioscience* 11.2 (2012), pp. 135–148.

[6] Ian F Akyildiz, Josep Miquel Jornet, and Massimiliano Pierobon. "Nanonetworks: A new frontier in communications". In: *Communications of the ACM* 54.11 (2011), pp. 84–89.

[7] IF Akyildiz et al. "The internet of bio-nano things". In: *IEEE Communications Magazine* 53.3 (2015), pp. 32–40.

[8] Tadashi Nakano et al. "Molecular communication among biological nanomachines: A layered architecture and research issues". In: *IEEE transactions on nanobioscience* 13.3 (2014), pp. 169–197.

[9] Baris Atakan, Ozgur B Akan, and Sasitharan Balasubramaniam. "Body area nanonetworks with molecular communications in nanomedicine". In: *IEEE Communications Magazine* 50.1 (2012).

[10] Adriano Cavalcanti et al. "Nanorobot communication techniques: A comprehensive tutorial". In: *Control, Automation, Robotics and Vision, 2006. ICARCV'06. 9th International Conference on*. IEEE. 2006, pp. 1–6.

[11] Yutaka Okaie et al. "Cooperative target tracking by a mobile bionanosensor network". In: *IEEE transactions on nanobioscience* 13.3 (2014), pp. 267–277.

[12] T Nakano et al. "Swarming biological nanomachines through molecular communication for targeted drug delivery". In: *SCIS-ISIS 2012* (2012).

[13] Patrick Couvreur and Christine Vauthier. "Nanotechnology: intelligent design to treat complex disease". In: *Pharmaceutical research* 23.7 (2006), pp. 1417–1450.

[14] Ming-Tang Chen and Ron Weiss. "Artificial cell-cell communication in yeast Saccharomyces cerevisiae using signaling elements from Arabidopsis thaliana". In: *Nature biotechnology* 23.12 (2005), pp. 1551–1555.

[15] Yoshihiro Sasaki et al. "A nanosensory device fabricated on a liposome for detection of chemical signals". In: *Biotechnology and bioengineering* 105.1 (2010), pp. 37–43.

[16] Tae Seok Moon et al. "Genetic programs constructed from layered logic gates in single cells". In: *Nature* 491.7423 (2012), pp. 249–253.

[17] Piro Siuti, John Yazbek, and Timothy K Lu. "Synthetic circuits integrating logic and memory in living cells". In: *Nature biotechnology* 31.5 (2013), pp. 448–452.

[18] Shuohao Huang and Masamichi Kamihira. "Development of hybrid viral vectors for gene therapy". In: *Biotechnology advances* 31.2 (2013), pp. 208–223.

[19] Achim Gossler et al. "Transgenesis by means of blastocyst-derived embryonic stem cell lines". In: *Proceedings of the National Academy of Sciences* 83.23 (1986), pp. 9065–9069.

[20] Paul D Robbins and Steven C Ghivizzani. "Viral vectors for gene therapy". In: *Pharmacology & therapeutics* 80.1 (1998), pp. 35–47.

[21] Octavio Mondragón-Palomino et al. "Entrainment of a population of synthetic genetic oscillators". In: *Science* 333.6047 (2011), pp. 1315–1319.

[22] Jared E Toettcher et al. "A synthetic–natural hybrid oscillator in human cells". In: *Proceedings of the National Academy of Sciences* 107.39 (2010), pp. 17047–17052.

[23] Lourdes Muñoz et al. "Mimicking insect communication: Release and detection of pheromone, biosynthesized by an alcohol acetyl transferase immobilized in a microreactor". In: *PloS one* 7.11 (2012), e47751.

[24] Marina Cole et al. "Towards a biosynthetic infochemical communication system". In: *Procedia Chemistry* 1.1 (2009), pp. 305–308.

[25] Mehmet S Kuran et al. "Modulation techniques for communication via diffusion in nanonetworks". In: *Communications (ICC), 2011 IEEE International Conference on*. IEEE. 2011, pp. 1–5.

[26] Adam Noel, Karen C Cheung, and Robert Schober. "Optimal receiver design for diffusive molecular communication with flow and additive noise". In: *IEEE transactions on nanobioscience* 13.3 (2014), pp. 350–362.

[27] Luis C Cobo and Ian F Akyildiz. "Bacteria-based communication in nanonetworks". In: *Nano Communication Networks* 1.4 (2010), pp. 244–256.

[28] Nariman Farsad et al. "On the capacity of diffusion-based molecular timing channels". In: *Information Theory (ISIT), 2016 IEEE International Symposium on*. IEEE. 2016, pp. 1023–1027.

[29] Yonathan Murin et al. "Time-slotted transmission over molecular timing channels". In: *Nano Communication Networks* 12 (2017), pp. 12–24.

[30] Pedro Cuatrecasas. "Membrane receptors". In: *Annual review of biochemistry* 43.1 (1974), pp. 169–214.

[31] VE Bochenkov and GB Sergeev. "Sensitivity, selectivity, and stability of gas-sensitive metal-oxide nanostructures". In: *Metal oxide nanostructures and their applications* 3 (2010), pp. 31–52.

[32] Marina Cole et al. "Biomimetic insect infochemical communication system". In: *Sensors, 2009 IEEE*. IEEE. 2009, pp. 1358–1361.

[33] Massimiliano Pierobon and Ian F Akyildiz. "A physical end-to-end model for molecular communication in nanonetworks". In: *IEEE Journal on Selected Areas in Communications* 28.4 (2010).

[34] Hamidreza Arjmandi et al. "Diffusion-based nanonetworking: A new modulation technique and performance analysis". In: *IEEE Communications Letters* 17.4 (2013), pp. 645–648.

[35] Vahid Jamali et al. "Channel Estimation for Diffusive Molecular Communications". In: *IEEE Transactions on Communications* 64.10 (2016), pp. 4238–4252.

[36] Satoshi Hiyama et al. "Biomolecular-motor-based autonomous delivery of lipid vesicles as nano-or microscale reactors on a chip". In: *Lab on a Chip* 10.20 (2010), pp. 2741–2748.

[37] Maria Gregori and Ian F Akyildiz. "A new nanonetwork architecture using flagellated bacteria and catalytic nanomotors". In: *IEEE Journal on Selected Areas in Communications* 28.4 (2010).

[38] Akihiro Enomoto et al. "Design of self-organizing microtubule networks for molecular communication". In: *Nano Communication Networks* 2.1 (2011), pp. 16–24.

[39] S Hiyama et al. "Molecular communication". In: *Journal-Institute of Electronics Information and Communication Engineers* 89.2 (2006), p. 162.

[40] Tadashi Nakano et al. "Molecular communication through gap junction channels: System design, experiments and modeling". In: *Bio-Inspired Models of Network, Information and Computing Systems, 2007. Bionetics 2007. 2nd.* IEEE. 2007, pp. 139–146.

[41] Michael Moore et al. "A design of a molecular communication system for nanomachines using molecular motors". In: *Pervasive Computing and Communications Workshops, 2006. PerCom Workshops 2006. Fourth Annual IEEE International Conference on.* IEEE. 2006, 6–pp.

[42] Andrew W Eckford. "Nanoscale communication with Brownian motion". In: *Information Sciences and Systems, 2007. CISS'07. 41st Annual Conference on.* IEEE. 2007, pp. 160–165.

[43] Andrew W Eckford. "Achievable information rates for molecular communication with distinct molecules". In: *Bio-Inspired Models of Network, Information and Computing Systems, 2007. Bionetics 2007. 2nd.* IEEE. 2007, pp. 313–315.

[44] Nariman Farsad, Weisi Guo, and Andrew W Eckford. "Tabletop molecular communication: Text messages through chemical signals". In: *PloS one* 8.12 (2013), e82935.

[45] Takuya Obuchi et al. "Inbody mobile bionanosensor networks through non-diffusion-based molecular communication". In: *Communications (ICC), 2015 IEEE International Conference on.* IEEE. 2015, pp. 1078–1084.

[46] Bon-Hong Koo et al. "Molecular MIMO: From theory to prototype". In: *IEEE Journal on Selected Areas in Communications* 34.3 (2016), pp. 600–614.

[47] Ling-San Meng et al. "MIMO communications based on molecular diffusion". In: *Global Communications Conference (GLOBECOM), 2012 IEEE*. IEEE. 2012, pp. 5380–5385.

[48] Reza Mosayebi et al. "Receivers for diffusion-based molecular communication: Exploiting memory and sampling rate". In: *IEEE Journal on Selected Areas in Communications* 32.12 (2014), pp. 2368–2380.

[49] Vahid Jamali et al. "Non-Coherent Multiple-Symbol Detection for Diffusive Molecular Communications". In: *Proceedings of the 3rd ACM International Conference on Nanoscale Computing and Communication*. ACM. 2016, p. 7.

[50] Deniz Kilinc and Ozgur B Akan. "Receiver design for molecular communication". In: *IEEE Journal on Selected Areas in Communications* 31.12 (2013), pp. 705–714.

[51] Ling-San Meng et al. "On receiver design for diffusion-based molecular communication". In: *IEEE Transactions on Signal Processing* 62.22 (2014), pp. 6032–6044.

[52] Bin Li et al. "Local convexity inspired low-complexity noncoherent signal detector for nanoscale molecular communications". In: *IEEE Transactions on Communications* 64.5 (2016), pp. 2079–2091.

[53] Burcu Tepekule et al. "A novel pre-equalization method for molecular communication via diffusion in nanonetworks". In: *IEEE Communications letters* 19.8 (2015), pp. 1311–1314.

[54] Sachin Kadloor, Raviraj S Adve, and Andrew W Eckford. "Molecular communication using brownian motion with drift". In: *IEEE Transactions on NanoBioscience* 11.2 (2012), pp. 89–99.

[55] Nariman Farsad et al. "On-chip molecular communication: Analysis and design". In: *IEEE Transactions on NanoBioscience* 11.3 (2012), pp. 304–314.

[56] Hamidreza Arjmandi et al. "Ion pump based bio-synthetic modulator model for diffusive molecular communications". In: *Signal Processing Advances in Wireless Communications (SPAWC), 2016 IEEE 17th International Workshop on*. IEEE. 2016, pp. 1–6.

[57] Na-Rae Kim, Andrew W Eckford, and Chan-Byoung Chae. "Symbol interval optimization for molecular communication with drift". In: *IEEE transactions on nanobioscience* 13.3 (2014), pp. 223–229.

[58] Adam Noel, Karen C Cheung, and Robert Schober. "Multi-scale stochastic simulation for diffusive molecular communication". In: *Communications (ICC), 2015 IEEE International Conference on*. IEEE. 2015, pp. 1109–1115.

[59] Arman Ahmadzadeh, Adam Noel, and Robert Schober. "Analysis and design of multi-hop diffusion-based molecular communication networks". In: *IEEE Transactions on Molecular, Biological and Multi-Scale Communications* 1.2 (2015), pp. 144–157.

[60] Adam Noel, Karen C Cheung, and Robert Schober. "Joint channel parameter estimation via diffusive molecular communication". In: *IEEE Transactions on Molecular, Biological and Multi-Scale Communications* 1.1 (2015), pp. 4–17.

[61] Nariman Farsad et al. "Channel and noise models for nonlinear molecular communication systems". In: *IEEE Journal on Selected Areas in Communications* 32.12 (2014), pp. 2392–2401.

[62] Massimiliano Pierobon and Ian F Akyildiz. "Noise analysis in ligand-binding reception for molecular communication in nanonetworks". In: *IEEE Transactions on Signal Processing* 59.9 (2011), pp. 4168–4182.

[63] Vahid Jamali et al. "SCW Codes for Optimal CSI-Free Detection in Diffusive Molecular Communications". In: *arXiv preprint arXiv:1701.06338* (2017).

[64] ME Orme and MAJ Chaplain. "A mathematical model of vascular tumour growth and invasion". In: *Mathematical and Computer Modelling* 23.10 (1996), pp. 43–60.

[65] Robert A Gatenby and Edward T Gawlinski. "A reaction-diffusion model of cancer invasion". In: *Cancer research* 56.24 (1996), pp. 5745–5753.

[66] Philip Nelson and Sebastian Doniach. "Biological physics: Energy, information life". In: *Physics Today* 57.11 (2004), pp. 63–64.

[67] Mohammad U Mahfuz, Dimitrios Makrakis, and Hussein T Mouftah. "A comprehensive study of sampling-based optimum signal detection in concentration-encoded molecular communication". In: *IEEE transactions on nanobioscience* 13.3 (2014), pp. 208–222.

[68] Adam Noel, Karen C Cheung, and Robert Schober. "Improving receiver performance of diffusive molecular communication with enzymes". In: *IEEE Transactions on NanoBioscience* 13.1 (2014), pp. 31–43.

[69] Ignacio Llatser, Eduard Alarcón, and Massimiliano Pierobony. "Diffusion-based channel characterization in molecular nanonetworks". In: *Computer Communications Workshops (INFOCOM WKSHPS), 2011 IEEE Conference on*. IEEE. 2011, pp. 467–472.